Title

A Limited Parametric Study of Reformate Gas Composition on a Reformate and Methane Bi-fueled Flame

Author

Horton, Michael

Publication Date

2022

Peer reviewed|Thesis/dissertation

A Limited Parametric Study of Reformate Gas Composition on a Reformate and Methane Bi-fueled Flame

By

MICHAEL HORTON

THESIS

Submitted in partial satisfaction of the requirements for the degree of

MASTER OF SCIENCE

in

Mechanical and Aerospace Engineering

in the

OFFICE OF GRADUATE STUDIES

of the

UNIVERSITY OF CALIFORNIA

DAVIS

Approved:

_____

Paul Erickson, Chair

_____

Vinod Narayanan

_____

Benjamin Shaw

2022

CONTENTS

ABSTRACT

A Limited Parametric Study of Reformate Gas Composition on a Reformate and Methane Bi-fueled Flame

A non-premixed, reformate and methane flame was experimentally and numerically investigated to explore the effect of steam to carbon ratio and reformate gas content on the criteria emissions generated. In order to better isolate the effects, the experiments were run at fixed flow rates and inlet temperatures. The steam to carbon ratio was varied from 2 to 3 while the reformate gas content was varied from 12.5% to 75% on a molar basis. Nitrogen oxide measurements were collected and analyzed to determine trends throughout the design space. Additionally, an OpenFOAM 2D model of the system was created, validated, and used to further investigate the system.

Chapter 1

Introduction

1.1 Motivation

Methane generation constitutes the largest share of power generation in the United States and current trends project growth in the consumption of the gas though 2050 [1]. In 2021, the United States alone consumed approximately 30 trillion cubic feet of natural gas. Figure 1. illustrates the current and future scope of natural gas usage in the United States.

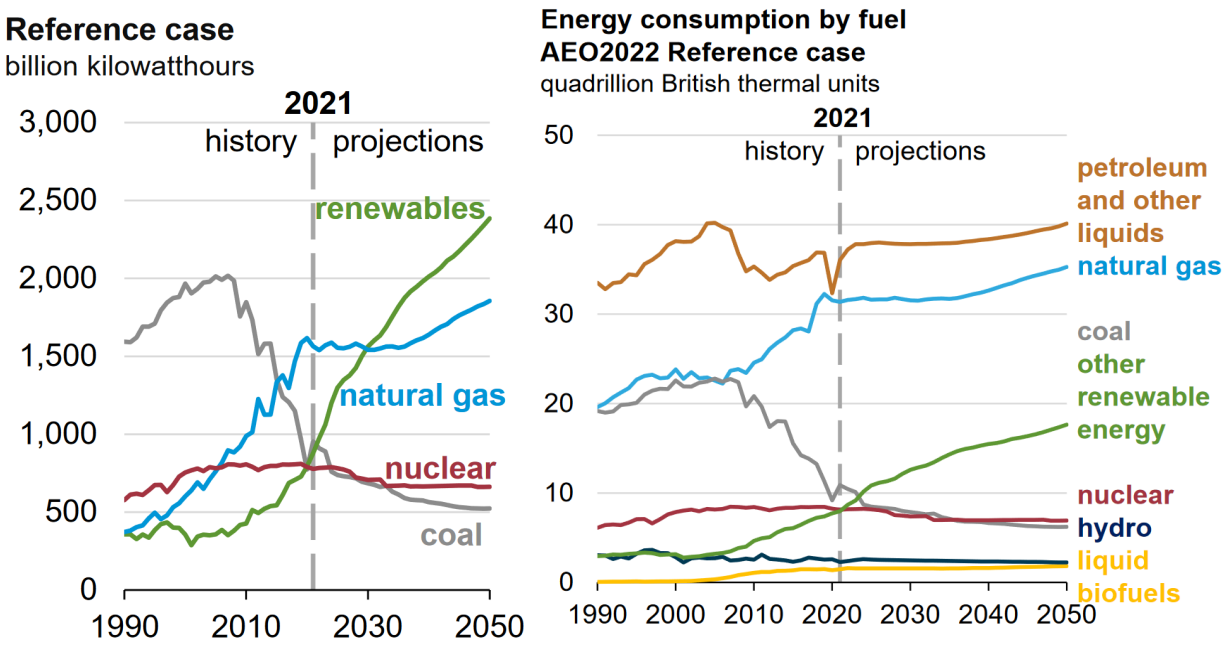

Figure 1: U.S. Electricity Generation by Source (Left) and U.S. Energy Consumption by Fuel (Right)[1]

With such a large hold on the energy sector, a small change in emissions or efficiency has the potential to cause a large change in global pollutant generation.

The EPA defines six criteria pollutants that have a significant impact on people and the environment: nitrogen oxides (NO_x) , sulfur oxides (SO_x), carbon monoxide (CO) , particulate matter, ozone , and lead [2]. Natural gas does not contain high concentrations of sulfur or lead so very little, if any, sulfur oxides or lead compounds are produced through combustion. Additionally methane does not form carbon particulates as much as many other fuels so the particulate matter emissions tend to be low. For these reasons, nitrogen oxides and carbon monoxide are the most relevant criteria pollutants in natural gas combustion [2].

NO_X generated from gas turbines in the United States is regulated based on standards from the “Stationary Gas and Combustion Turbines: New Source Performance Standards” (NSPS) produced by the EPA. This document categorizes and addresses natural gas turbines based on maximum heat input. The allowable NO_X emissions for each class of turbine is defined by Subpart KKKK of part 60 and is shown below in Table 1.

Table 1. Stationary Gas and Combustion Turbine Emission Standards [3]

Combustion turbine type	Combustion turbine heat input at base load rating (HHV)	NO_X emissions standard	Alternate NO_X emissions standard in ppm at 15 percent O_2
New turbine firing natural gas, electric generating	≤ 15 MW (50 MMBtu/h)	67 ng/J (0.16 lb/MMBtu) heat input or 290 ng/J of gross energy output (2.3 lb/MWh).	42
New turbine firing natural gas, mechanical drive	≤ 15 MW (50 MMBtu/h)	160 ng/J (0.37 lb/MMBtu) heat input or 690 ng/J of gross energy output (5.5 lb/MWh).	100
New turbine firing natural gas	> 15 MW (50 MMBtu/h) and ≤ 250 MW (850 MMBtu/h).	40 ng/J (0.093 lb/MMBtu) heat input or 150 ng/J of gross energy output (1.2 lb/MWh).	25
New, modified, or reconstructed turbine firing natural gas.	> 250 MW (850 MMBtuh).	24 ng/J (0.056 lb/MMBtu) heat input or 54 ng/J of gross energy output (0.43 lb/MWh).	15
New turbine firing fuels other than natural gas, electric generating.	≤ 15 MW (50 MMBtu/h)	160 ng/J (0.38 lb/MMBtu) heat input or 710 ng/J of gross energy output (5.6 lb/MWh).	96
New turbine firing fuels other than natural gas, mechanical drive.	≤ 15 MW (50 MMBtu/h)	250 ng/J (0.59 lb/MMBtu) heat input or 1,100 ng/J of gross energy output (8.7 lb/MWh).	150
New turbine firing fuels other than natural gas	> 15 MW (50 MMBtu/h) and ≤ 250 MW (850 MMBtu/h).	120 ng/J (0.29 lb/MMBtu) heat input or 470 ng/J of gross energy output (3.7 lb/MWh).	74
New, modified, or reconstructed turbine firing fuels other than natural gas.	> 250 MW (850 MMBtu/h).	73 ng/J (0.17 lb/MMBtu) heat input or 160 ng/J of gross energy output (1.3 lb/MWh).	42
Modified or reconstructed turbine	≤ 15 MW (50 MMBtu/h)	250 ng/J (0.59 lb/MMBtu) heat input or 1,100 ng/J of gross energy output (8.7 lb/MWh).	150
Modified or reconstructed turbine firing natural gas.	> 15 MW (50 MMBtu/h) and ≤ 250 MW (850 MMBtu/h).	67 ng/J (0.16 lb/MMBtu) heat input or 250 ng/J of gross energy output (2.0 lb/MWh).	42
Modified or reconstructed turbine firing fuels other than natural gas.	> 15 MW (50 MMBtu/h) and ≤ 250 MW (850 MMBtu/h).	160 ng/J (0.38 lb/MMBtu) heat input or 600 ng/J of gross energy output (4.8 lb/MWh).	96

There are a handful of systems which currently exist to reduce natural gas turbine NO_X emissions. These include humid air/ steam injected turbines, Premixed Lean combustors, lean head end combustors.[4][5] Methods such as hydrogen and natural gas bi-fueling have additionally been investigated as potential solutions for emission reduction. Hydrogen addition has been shown to drastically increase the flame speed and reduce the lean operating conditions of fuel mixtures. This improves the flame stability and reduces CO emissions[6][7][8]. The higher temperatures generated in a hydrogen methane blend, however, can produce more NO_x. To combat this, steam can also be injected into the system. When combined, the blend of methane, steam, and hydrogen has experimentally shown a decrease in CO emissions with only a small increase in NO_x[9]. Hydrogen has also been shown to reduce radicals that lead to the production of prompt NO_x. [10]

Preliminary research has been conducted on the inclusion of reformate gas generated from a methane feedstock in a diffusion methane flame. The experiment conducted showed that NO_x emissions can be reduced significantly by adding reformate gas to a methane flame. Figure 2 below shows a large reduction in NO_x emissions resulting from an addition of reformate gas[11].

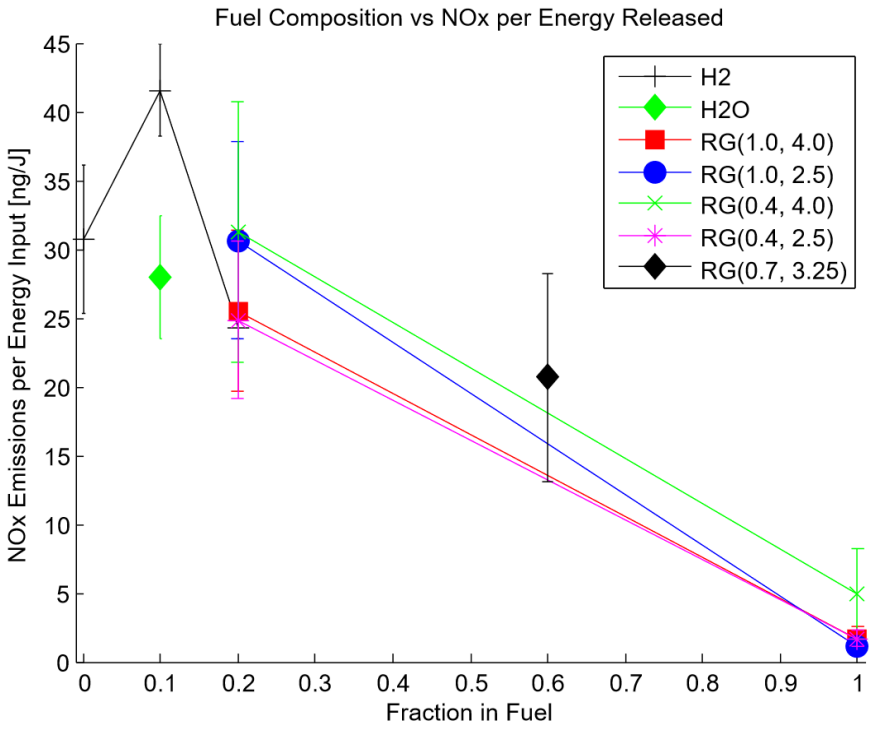

Figure 2. Previous Emissions Results of Reformate-Methane Flame[11]

1.2 Problem Definition

Both hydrogen and water addition have been shown to alter the burning characteristics of methane in unique and potentially beneficial ways. Despite this, there is very little research on the combustion characteristics of reformate gas and methane blends. The small number of existing studies are typically based on syngas generated from other feedstocks, such as coal, and typically have a much higher concentration of carbon monoxide compared to methane generated reformate gas. To better understand the emissions characteristics and better predict the effects of reformate gas inclusion in natural gas systems, combustion of reformate gas and methane blends should be investigated.

1.3 Research Objectives

The objectives of this investigation are to quantify critical composition parameters of a reformate-methane blend and to investigate their emissions characteristics. A laminar, co-flow, diffusion flame, operating in an ambient pressure and elevated temperature environment, will be experimentally and numerically investigated to determine the significance of the chosen parameters as well as to determine trends in the emissions produced.

Chapter 2

Literature Review

In this section, a thorough literature review was conducted in order to provide relevant precursory information on chemical mechanisms and trends observed through experimentation that were used as a basis for this study. Additionally, the section gives insight on how modern systems manage NO_X emissions.

2.1.1 Hydrogen

There are a number of problems that come with the usage of hydrogen as a fuel source. The most pertinent of which being storage and transportation. At ambient conditions, the density of hydrogen is significantly lower than that of any other fuel. As a result, the density needs to be increased in order to store it in an economically efficient volume. The most common form of storage, compression, utilizes high pressure tanks to contain the hydrogen. To increase the density as much as possible, tanks maximum operating pressures range from 20 - 80 MPa [12]. These tanks are heavy and expensive compared to lower pressure tanks built for other gaseous fuels. In addition to the bulky tanks, the compression process requires a significant amount of power. Compressing one kilogram of hydrogen, isothermally, from average atmospheric conditions to 80 MPa requires 2.21 kW*hr [13].

The other major storage technique used is liquefaction. Liquefaction systems cool the hydrogen to approximately 21 K, where hydrogen is a liquid at atmospheric pressure. Just like compression, this process consumes a large amount of power. One kilogram of hydrogen requires 3.23 kW*hr of energy in an ideal system to be liquified [13]. Another problem with liquefaction systems is that the liquid hydrogen is lost over time. Even in well insulated systems

a small amount of energy is passed through the tank walls into the liquid. The resulting boil off is often vented into the atmosphere as closed systems would need to operate as high as 1000 MPa in order to store the liquid hydrogen at room temperature.

To avoid storing hydrogen, hydrogen is often generated on site. The two most common methods of generation include the reformation of hydrocarbons and electrolysis. Electrolysis uses water as the source of hydrogen atoms. In this process electrical power is used to separate the hydrogen atoms from the oxygen in the water molecule. In reformation, hydrocarbons and water act as the hydrogen source. The hydrogen atoms are removed from the source molecules by running them over a catalyst at high temperatures. Electrolysis accounts for approximately 4% of the hydrogen produced globally while reformation accounts for 96% [14]

2.1.2 Methane Steam Reformation

Methane steam reformation (MSR) is a common and cost effective method of producing hydrogen. Over 50% of the world's hydrogen production is based on the MSR process[15]. Reformation, in general, is a chemical process in which a hydrocarbon is broken down into a hydrogen rich product. This process typically utilizes a catalyst bed to lower the temperature required to reform the hydrocarbon and shift the equilibrium to produce more desirable products. In MSR, methane is typically combined with steam and passed over two sets of catalysts. The CH4 is first broken down into H_2 and CO in the first reactor. The initial reactors are filled with high temperature catalysts typically made of chromium and iron oxide. These catalysts operate best in the 300-400 °C range [16]. Once passed through the first reactor the CO reacts with H_2O through the water gas shift reaction to produce H_2 and CO_2 in a water gas

shift reactor. These reactors operate using lower temperature catalysts, such as copper promoted zinc oxide, that can run at as low as 100 °C [17]. The global reforming and water gas shift reactions and their respective heat of reactions are shown in eqn. 2.1 and 2.2.

$$CH_4 + H_2O \leftrightarrow CO + 3H_2 \quad (2.1)$$

$$CO + H_2O \leftrightarrow CO_2 + H_2 \quad (2.2)$$

The first step of this process is highly endothermic while the water gas shift is slightly exothermic. The result of the two reactions is a global net endothermic reaction.

$$CH_4 + 2H_2O \leftrightarrow CO_2 + 4H_2 \quad (2.3)$$

2.2 Combustion of fuels

2.2.1 Methane Combustion

The first step in methane combustion involves separating a hydrogen radical from the CH_4 to produce a CH_3 radical. This can happen spontaneously at high enough temperatures or can happen though the pathways shown in Eq 2.4 and Eq2.5, sourced from the GRI-3.0 mechanism. The variable X in these equations is a radical generated in the flame typically, H, OH, O, or HO_2. For each of the following equations describing a chemical reaction an annotation, shown as (rxnY), is given. Where Y is a number corresponding to the reaction number of the described equation in the GRI-3.0 mechanism.

$$CH_4 + O_2 \leftrightarrow CH_3 + HO_2 \,(rxn117) \quad (2.4)$$

$$CH_4 + X \leftrightarrow CH_3 + HX(rxn10, rxn52, rxn97, rxn156) \quad (2.5)$$

Once broken down into CH_3 , the hydrocarbon further reacts with the radicals described in Eq. 2.5 to form CO. If enough oxidizer is present in the reaction zone, the CO reacts with oxygen to form CO_2.

2.2.2 H_2 Combustion

For hydrogen combustion the initiating reactions are:

$$H_2 + M \leftrightarrow 2H + M \ (rxn\ 38) \tag{2.6}$$

$$H_2 + O_2 \leftrightarrow H + HO_2 \ (rxn44) \tag{2.7}$$

Radicals produced from these reactions further react to produce a large pool of H, OH and O radicals. These radicals continue to react with the H_2, O_2 and H_2O present in the reaction zone. The reactions continue until finally terminating the chain reaction through one of the reactions below in Eq 2.8-11.

$$2H + M \leftrightarrow H_2 + M \ (rxn\ 38) \tag{2.8}$$

$$2O + M \leftrightarrow O_2 + M \ (rxn\ 0\ ) \tag{2.9}$$

$$H + O + M \leftrightarrow OH + M \ (rxn\ 1) \tag{2.10}$$

$$H + OH + M \leftrightarrow H_2O + M \ (rxn\ 42) \tag{2.11}$$

2.3 NO_x formation

2.3.1 Thermal NO_x

The first of the NO_x sources is thermally generated NO_x, commonly called the Zeldovich mechanism. Thermally generated NO_x tends to be the leading source of NO_x in a natural gas

turbine . The mechanism is characterized by the relatively large activation energy of the initiating reaction described in Eq 2.12. [15][19][20][21].

$$N_2 + O \leftrightarrow NO + N\,(rxn\,177) \qquad k1f = 2.7 \times 10^{13} e^{-355/RT} \qquad (2.12)$$

$$N + O_2 \leftrightarrow NO + O\,(rxn\,178) \qquad k2f = 9.0 \times 10^{9} T\ e^{-6500/RT} \qquad (2.13)$$

$$N + OH \leftrightarrow NO + H\,(rxn\,179) \qquad k3f = 3.36 \times 10^{13} e^{-385/RT} \qquad (2.14)$$

The rate limiting step shown in Eq 2.12 is much slower than that shown in Eq 2.13. As seen in k1f in Eqn 1.12, the rate limiting step is dependent on temperature. This mechanism is negligible at low temperatures but after approximately 1500°C, the production of NO_x rapidly increases. Overall, this mechanism is very slow when compared to other combustion reactions. [15] As such, in combustion systems, the final proportion of NO_x generated through this mechanism is highly dependent on the nitrogen and oxygen mixture's residence time in elevated temperature environments.

2.3.2 Prompt NO_x

Another source of NO_x is through the radicals in a flame. This mechanism is often called prompt NO or the Fenimore mechanism. The initiating reaction is described in Eq 2.15.

$$CH + N_2 \leftrightarrow HCN + N \qquad (2.15)$$

The reaction does not have a large dependence on temperature, and requires CH_x radicals. This results in the mechanism operating only in the flame front. The prompt reactions also act on a much shorter timescale than the zeldovich mechanism and are thus much less dependent on residence time of hot exhaust in a combustion chamber.

2.3.3 Fuel Bound NO_x

The final source is fuel-bound NO_x. This NO_x is produced from nitrogen species, typically ammonia, in the fuel. In a standard diffusion flame, most of the fuel-bound nitrogen will react in the flame and create NO_x. It is possible to reduce the conversion of fuel-bound nitrogen into NO_x using rich-lean combustors, but the best method found to reduce this form of NO_x production is cleaning the fuel of nitrogen species before combustion.

2.4 CO Formation

Carbon monoxide is a common intermediate in hydrocarbon combustion. In a complete combustion all of the CO that is generated is oxidized to form CO_2. The oxidation of carbon monoxide is a critical step in the combustion of hydrocarbons and often is the step that produces the majority of the energy.The bulk of the CO that ends up being exhausted is a result of incomplete combustion, typically caused by low oxygen levels, low mixing, quenching, or poor flame stability.

2.5 Premixed Flames

A premixed flame is a flame in which the fuel and oxidizer are combined before the combustion. As the chemical components required to generate a flame are well mixed in this scheme there are smaller changes in local stoichiometry vs diffusion flames. In this category the combustion reactions occur throughout the fuel-air domain. This allows for control over the local air to fuel ratio that regions of the flame combust.

2.6 Diffusion Flames

In a diffusion flame the fuel and the oxidizer are not combined before burning. The rate of combustion is limited to the rate at which oxidiser can diffuse into the flame. As the fuel only interacts with the oxidiser on the boundaries of the two domains, the combustion takes place on the surface of the fuel domain[22]. This phenomenon is shown in Figure 3. where the fuel domain is located between the flame fronts, where the fuel concentration is highest. Many older natural gas turbine burners are based on diffusion flames as the fuel and the air are injected into the reaction zone directly without prior mixing [5].

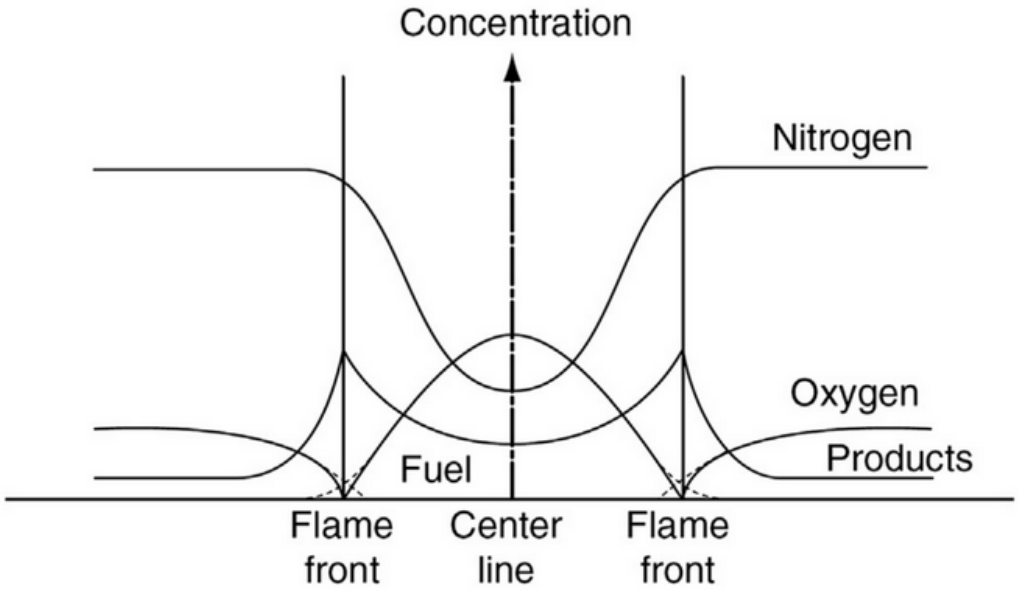

Figure 3. Diffusion Flame Diagram[22]

2.7 NO_x control schemes

2.7.1 Wet control systems

The oldest mainstream system that was developed for combating NO_x was the water injected system [5]. These systems use water as a diluent in the combustion chamber. The added water absorbs energy and reduces the flame temperature. The proportion of water in a fuel system is limited, however, based on how much can be added before the flame blows out. This acts as a limit on how far emissions can be reduced with this technique.

In most heat engines reducing the peak temperature of the cycle lowers the isentropic efficiency. In real natural gas brayton cycle or combined cycle power plants, however, the material used to build the system limits the allowed peak temperatures and thus efficiency. In these systems hot combustion gasses must be cooled to prevent melting or creeping out of tolerance of the turbine blades. With modern systems utilizing strengthened single crystal nickel-base superalloys, combustion products still must be cooled below 1800 - 1600 °C. [23] Water injection stops the combustion temperatures from reaching this high temperature without having to add as much excess air. As a result, the addition of water does not affect the thermal efficiency nearly as much as it would if the combustion gasses did not already have to be cooled.

2.7.2 Lean Head End Combustors

Another technology that is used in industry is the lean head end combustor. These systems are based around standard diffusion flame burners. The combustion chamber, however, is modified to actively inject air into the flame. This leans the average stoichiometry of the combustion, cooling the flame. As most natural gas turbines already compress large

amounts of excess air it is possible to inject this air later into the flame to lean the flame. This process reduces the flame temperature and shortens the length of the flame, reducing the residence time of the nitrogen and oxygen mixture in high temperature environments [5]

2.7.3 Lean Premix staged burners

One of the most common modern methods of NO_x emission reduction is the usage of lean premix staged burners. In these systems, the air and fuel is well mixed in a primary stage and is then sent to a secondary stage where it is combusted. In this second stage additional air can be injected into the flame to further lean the flame. By premixing the flame, manufacturers are able to alter the air to fuel ratio of the combustion easily. Increasing the air to fuel ratio causes the flame to burn lean, reducing the flame temperature. Achieving optimal performance from these systems, however, is not as simple as other methods. To reduce the emissions as much as possible the fuel has to be burning near the lean operating limit. Changes in combustor temperature, fuel flow, or air humidity can quickly extinguish a flame running close to these limits. [4][2]

2.8 Hydrogen Enriched Methane Combustion

One problem that arises with emission reduction methods such as lean premixed combustion is that methane is susceptible to blow out in highly strained or lean conditions. This is due to methane's relatively low flame speed and high ignition temperature. Inversely, hydrogen has a high flame speed and low ignition temperature. In addition to this, hydrogen has a wide flammability limit and can combust in very lean conditions. When methane is blended with hydrogen it has been shown that the hydrogen significantly improves the flammability limits and lean operating limits of the methane. The increase in flame stability has been exploited to push the lean limits of burners allowing for greater reduction of NO_x [24].

Chapter 3

Experimental Methods

3.1 Objectives

Based on previous works, such as Hwang's "*Blowout and Emissions Characteristics Evaluation of Methane Steam Reformate Gas*"[11], detailing significant positive benefits of adding reformate gas to a methane fuel stream, experiments were designed to further investigate how reformate gas composition and concentration alter emission characteristics. The experiments specifically were designed to study the NO_x emissions. Independent variables in this study included the steam to carbon ratio and the percentage of reformate gas in the blend. Other parameters such as inlet gas temperature, inlet air humidity, and fuel flow rate were held fixed. The measured dependent variable was the volumetric NO_x concentration in the exhaust.

3.2 Substitute Reformate Gas

To improve the run to run variation in gas blend composition, a representative reformate gas was produced. When reforming methane there are three important system parameters that determine the final reformate composition. These parameters include conversion, CO_2 selectivity, and steam to carbon ratio.

Conversion is the metric defining the proportion of methane broken down in the system. This metric is independent of the hydrogen yield as the methane decomposition has multiple stable pathways it can end in besides the ideal CO_2 and H_2. The most common of these pathways ends with unreacted water and CO. In these sets of experiments conversion was

taken to be 100%. This was assumed as the conversion would only add a constant scaling factor on the reformate gas ratio, a parameter that was changed as an independent variable. The inclusion of conversion would not affect the relative ratios of H_2 to CO, CO_2, or H_2O in the representative reformate gas.

The next metric, CO_2 selectivity, is based on the proportion of CO_2 vs CO that is generated. It is defined below in eqn 3.1

$$CO_2 selectivity = \frac{[CO_2]}{[CO] + [CO_2]} \quad (3.1)$$

To determine an accurate CO_2 selectivity to use for these experiments, selectivity was analyzed from a master's thesis paper from the Energy Research Laboratory at UC Davis [25]. The experiments conducted in this paper utilized a pelletized copper-zinc catalyst on an alumina substrate, branded FCRM-2. This data suggests that a CO2 selectivity of 96.2% was a realistic value to use.

The final parameter important to the reformate gas composition is the steam to carbon ratio. This is defined by the ratio of moles of water over moles of methane input into the reformer. The stoichiometric ratio, or ideal steam to carbon ratio, for MSR is two moles of water per one mole of water. This ratio is the ideal ratio that would make the system most energy efficient, however almost all steam reformation is done at higher steam to carbon ratios than stoichiometric. In practice more H_2O is added to prevent coking, carbon build up, from reducing the efficiency and conversion of the system. The added water, however, requires additional power to vaporize and overall reduces the efficiency of the reformer so lower steam to carbon ratio

Under ideal conditions the steam and methane would completely react forming hydrogen and carbon dioxide as shown in Eq 3.2.

$$CH_4 + 2H_2O \leftrightarrow 4H_2 + CO_2 \quad (3.2)$$

When taking CO_2 selectivity into account, however, there is CO and H_2O that is passed through the system. Shown in Eq 3.3 is the global reaction, under stoichiometric steam to carbon ratio, of MSR with a CO_2 selectivity of 96.2%.

$$CH_4 + 2H_2O \leftrightarrow 3.962H_2 + 0.038CO + 0.962CO_2 + 0.038H_2O \quad (3.3)$$

The global reaction equation becomes Eq. 3.4 when the steam to carbon ratio, denoted X2 is applied.

$$CH_4 + X2H_2O \leftrightarrow 3.962H_2 + 0.038CO + 0.962CO_2 + \ldots \quad (3.4)$$

$$\ldots (0.038 + X2 - 2)H_2O$$

3.3 Reformate Gas Ratio

The reformate gas ratio in this study was defined as the ratio of reformate gas to fuel on a molar basis. Examples of the ideal experimental fuel compositions calculated from chosen reformate gas ratios and steam to carbon ratios are displayed in Table 2.

Table 2. Ideal Experimental Fuel Compositions

Reformate Gas Ratio	Steam to Carbon Ratio	CH_4	H_2	CO	CO_2	H_2O
12.5	2	87.50%	9.90%	0.10%	2.40%	0.10%
75	2	25%	59.43%	0.57%	14.43%	0.57%
12.5	3	87.50%	8.25%	0.08%	2%	2.16%
75	3	25%	49.52%	0.47%	12.02%	12.97%

3.4 Dependent Variables

NO_x emissions are initially reported by the sensor as an average volumetric concentration, in parts per million, of the dry exhaust. To better compare these results to regulated emissions and to better compare configurations in this study, the NO_x concentrations were normalized to be in terms of nanograms of NO_x per Joule of methane input into the simulated system. In this study, the CH_4 energy input was based on both the CH_4 that was directly burned as well as the theoretical CH_4 feedstock used for producing the reformate gas. The measured value of NO_x in ppm is denoted by Y, the reformate gas ratio denoted by X1, and steam to carbon ratio denoted by X2.

The inlet volumetric flow rates are known for this system:

$$\dot{V}_{fuel} = 0.166\ standard\ liters\ per\ second$$

$$\dot{V}_{air} = 5\ standard\ liters\ per\ second$$

The ideal gas law is used to convert from a volumetric flow rate to a molar flow rate.

For all calculations T = 300 K and P = 101.3 kPa is assumed.

$$\dot{n} = \frac{P\dot{V}}{RT} = \dot{V} * 0.0406 \qquad (3.5)$$

Where $\dot{n}$ is in moles/second and $\dot{V}$ is in standard liters per second. The volumetric flow rate of air is passed into Eq 3.6 To calculate the molar flow rate of air entering the system.

$$\dot{n}_{air} = \dot{V}_{air} * 0.0406 \qquad (3.6)$$

The volumetric flow rate of methane is calculated by multiplying the volumetric flow rate of fuel by the ratio of methane to reformate gas. This factored into Eq 3.5 Results in Eq 3.7.

$$\dot{n}_{CH_4} = \dot{V}_{fuel} * (1 - X1) * 0.0406 \quad (3.7)$$

A factor C is defined as the total number of moles of gas created from the reformation of one mole of methane. This is used to determine the molar ratios of each reformate gas species.

$$C = 3.96 + 0.038 + 0.962 + (0.038 + X2 - 2) \quad (3.8)$$

Next the molar flow rates for carbon dioxide, carbon monoxide and hydrogen are calculated.

$$\dot{n}_{CO_2} = \frac{0.962}{C}\dot{V}_{fuel} * X1 * 0.0406 \quad (3.9)$$

$$\dot{n}_{CO} = \frac{0.038}{C}\dot{V}_{fuel} * X1 * 0.0406 \quad (3.10)$$

$$\dot{n}_{H_2} = \frac{3.96}{C}\dot{V}_{fuel} * X1 * 0.0406 \quad (3.11)$$

The NO_x analyser requires that the water be removed from the sample so in the equation the molar flow rate of water in the exhaust needs to be subtracted.

Complete combustion is assumed at this step. There was going to be some fuel that does not burn fully, or forms different products but the concentrations of these species are low enough to be insignificant. Eq 3.12 shows the complete combustion of the hydrogen in the system.

$$2H_2 + O_2 -> 2H_2O \quad (3.12)$$

For every mole of hydrogen in the fuel, one and a half moles of reactant get used and zero moles of the product make it to the NO_x analyser. The result is that the hydrogen accounts for a change in molecular flow rate, inside the system, of -0.5 $\dot{n}_{H_2}$. One $\dot{n}_{H_2}$ is added to the

system, one and a half $\dot{n}_{H_2}$ of reactants gets consumed during combustion and 0 $\dot{n}_{H_2}$ of dry product gets sent to the sensor.

The complete combustion of CO and CH_4 also need to be taken into account.

$$2CO + O_2 -> 2CO_2 \quad (3.13)$$

$$CH_4 + 2O_2 -> CO_2 + 2H_2O \quad (3.14)$$

For every mole of carbon monoxide in the fuel, one and a half moles of reactant get used and one mole of the product makes it to the NO_x analyser. The CO provides a net change in molar flow rate in the system of $0.5\dot{n}_{CO}$ .For every mole of methane in the fuel, three moles of reactant get used and one mole of products makes it to the NO_x analyser. Thus the CH_4 provides a net change in molar flow rate in the system of $-1\dot{n}_{CH_4}$. The molar flow rate of dry exhaust can then be calculated

$$\dot{n}_{ex,dry} = \dot{n}_{air} - 0.5\dot{n}_{H_2} - \dot{n}_{CH_4} + 0.5\dot{n}_{CO} + \dot{n}_{CO_2} \quad (3.15)$$

To calculate the mass flow rate of NO_x from the molar flow rate, the molecular weight of the NO_x must be known. NO_x, however, does not have one molecular weight that can be used as it is a grouping of both NO and NO_2. NO_2 is typically the dominant species in NO_x, so for this calculation the molecular weight of NO_2 is used. The resulting equation is

$$\dot{m}_{NO_x} = \dot{n}_{ex,dry} * 46(g//mol) * Y * 10^{-6} \quad (3.16)$$

The power, denoted by P , corresponding to the inlet stream of methane is based on both the molar flow rate of methane into the burner as well as the molar flow rate of hydrogen.

As 3.96 moles of hydrogen are generated for every mole of methane input into the reformer, the total methane input into both the burner and reformer would be

$$\dot{n}_{CH_4-inlet} = \dot{n}_{CH_4} + \frac{\dot{n}_{CH_4}}{3.96} \quad (3.17)$$

To calculate the power associated with the inlet methane, the molar flow rate of methane is multiplied by its molecular weight and by its lower heating value as shown in Eq 3.18.

$$P_{CH_4} = \dot{n}_{CH_4-inlet} * 16(g/mol) * 50.0(MJ/kg) \quad (3.18)$$

Finally, to normalize the NO_x emissions, the mass flow rate of NO_x exiting in the dry exhaust is divided by the power associated with the inlet methane.

$$Y_{Normalized} = \frac{\dot{m}_{NOx}}{P_{CH_4}} \quad (3.19)$$

3.5 Experimental Set-up

The experiments were conducted in a standalone system set up in the laboratory. As shown in Figure 4, the combustion chamber of the system was composed of a long square ventilation shaft that was held upright by lengths of slotted galvanized steel. This shaft was sealed on both ends with an adapter to convert from the square shaft to a 6 inch ventilation hose. The hose located on the top of the system transported the exhaust gas out of the combustion chamber into the fume extractor, while the hose located below the square shaft was connected to the air supply. Figure 6. and below shows the full system diagram, illustrating how each subsystem interacted with the system as a whole.

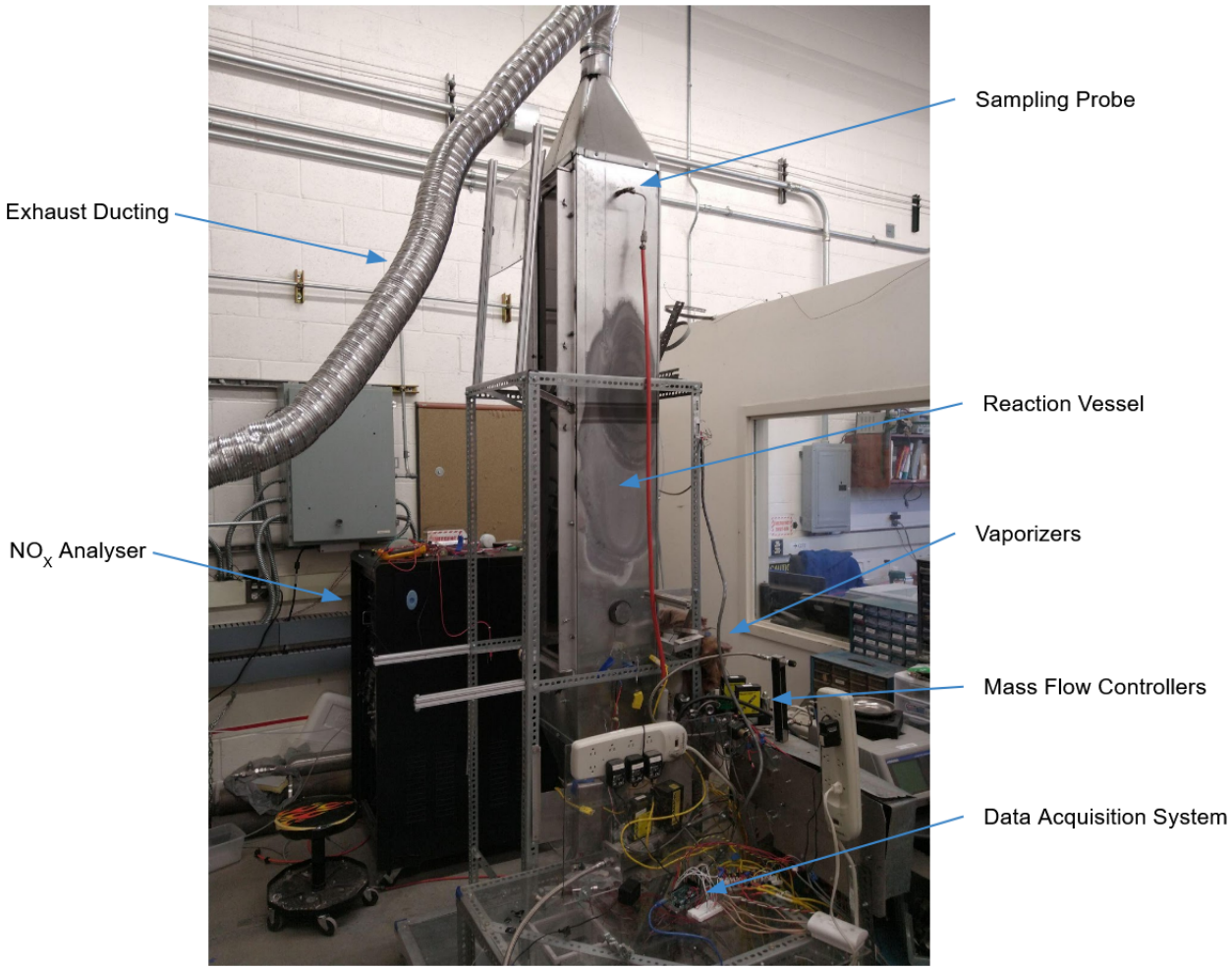

Figure 4. Experimental Facility

The main reaction vessel was a 2m long square ventilation shaft. Inside the vessel was a mixing chamber, air straightener, fuel nozzle, sampling probe, and a thermocouple. The relative locations of these parts are shown in Figure 5. The air straightener consisted of a 50mm thick aluminum honeycomb and was used to ensure air uniformity throughout the experiments. The sampling probe was located in the middle of the ventilation shaft, 1370mm above the fuel nozzle.

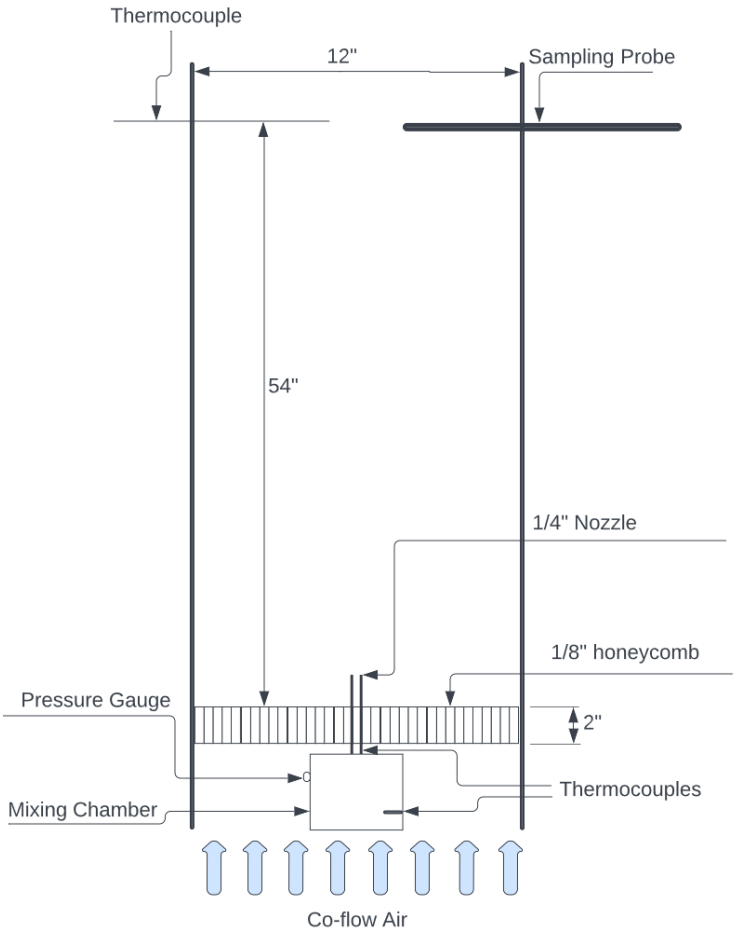

Figure 5. Combustion Chamber Layout

3.5.1 Fuel Supply

Each component of the fuel was supplied from size T(~300cf) compressed gas cylinders. The hydrogen, carbon monoxide,and methane was supplied from Praxair and was 99.995% purity, 99.5% purity, and 99.0% purity respectively. The CO_2 used was a 40%CO2, 60% methane blend. Each of these gasses were regulated down from tank pressures to approximately 200 kPa.

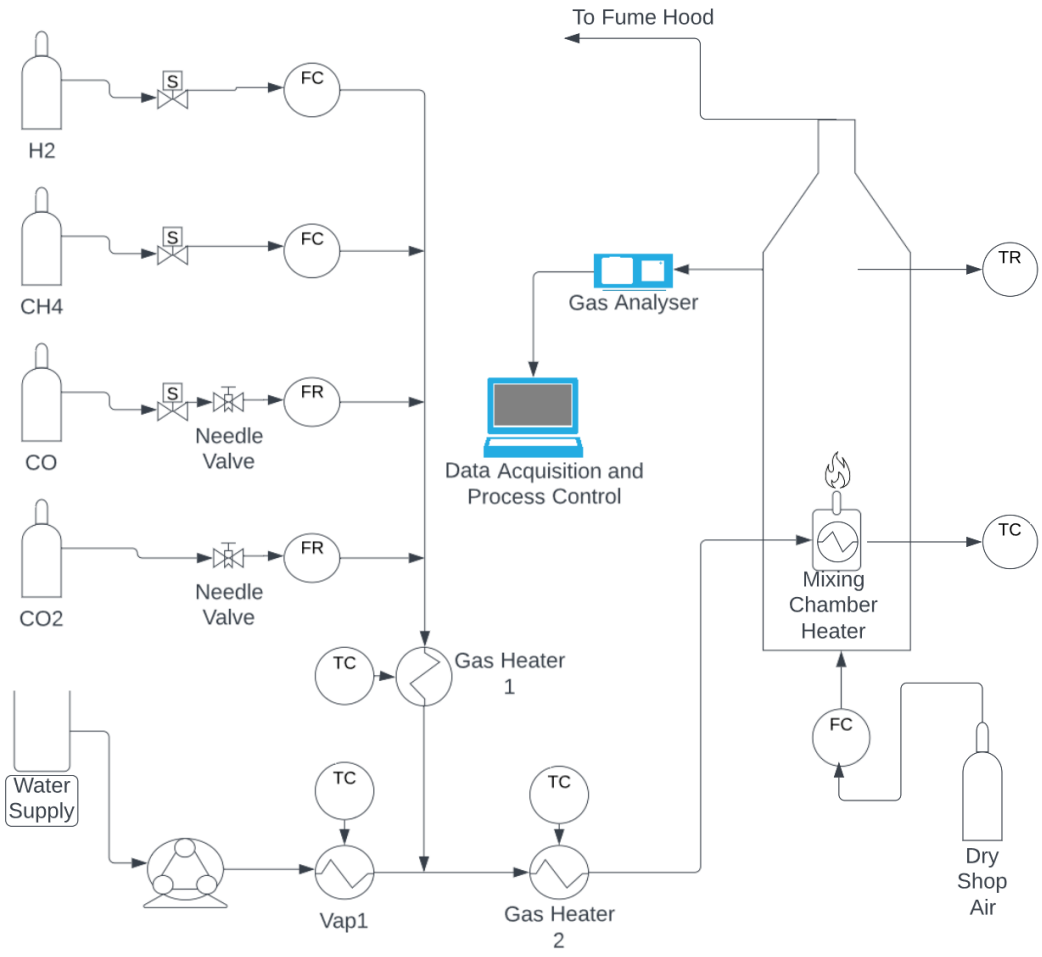

Figure 6. System Layout

Water was added to the fuel to simulate excess water from a methane steam reforming process. Deionized water was pumped into the vaporizer subsystem using a Cole-Parmer 7533-80 pump working with a Cole-Parmer 7013-20 peristaltic pump head. Water was pumped from a flask resting on a scale into the system. The scale readings were used to verify that the system was metering the flow at the desired rates. A MegaMoto Plus motor controller was used to control the speed of the pump

3.5.2 Air Supply

Pressurized air was supplied from an air compressor located inside the building. This air was regulated down to 200 kPa before being plumbed to the systems that required it. The air was measured to be consistently 11.9% relative humidity at 23.0C with a Fisher Scientific Traceable(R) hygrometer.

3.5.3 Vaporizers and Gas Heating

The water was vaporized by passing the metered stream of deionized water through a 10in, schedule-40, 304 stainless steel pipe that was heated with an internal cartridge heater. A diagram of this assembly is shown in Figure 7. The pipe was additionally filled with 1/16in steel shot to aid in heat transfer. To prevent surging, the water was pre-heated to 95 C in the first stage of the vaporizer and was fully vaporized further down the system .

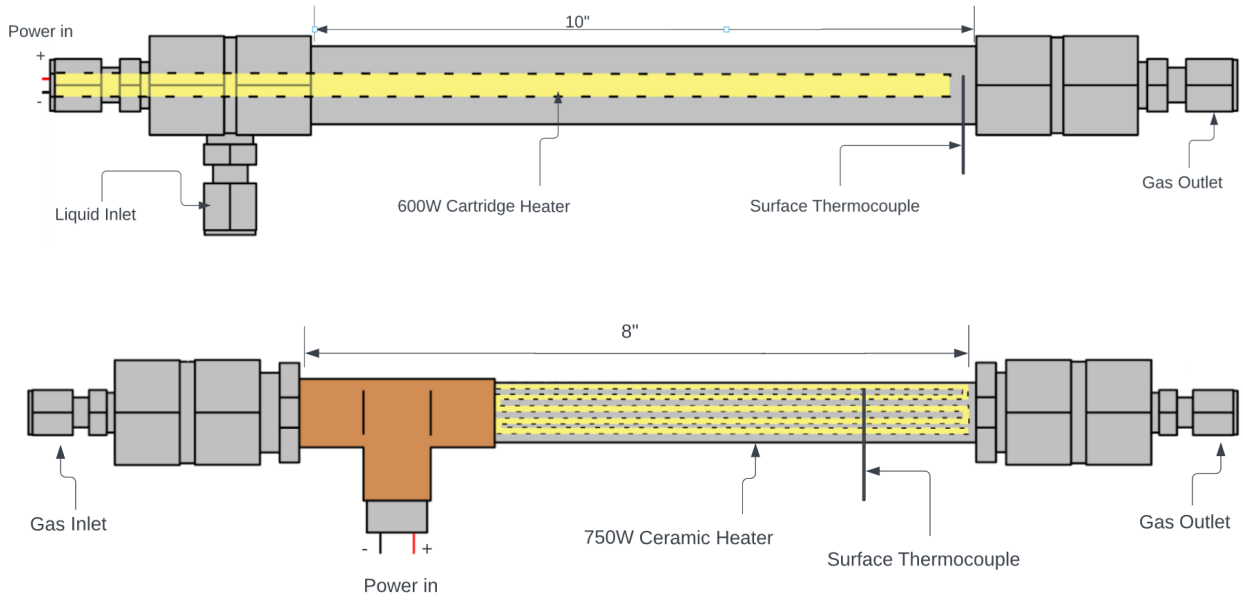

Figure 7. Vaporizer and Gas Heater Assemblies

The fluid heaters were oriented vertically on the back side of the system as shown in Figure 8. In this system the dry fuel passed through the first gas heater before being combined with the preheated water. The fuel water blend then was passed through an additional heater before being sent into the mixing chamber. The piping diagram for this layout can be seen above in Figure 6.

Figure 8. Vaporizers Installed on System

In addition to the vaporizers and gas heaters, the gas was heated in a large mixing chamber located directly below the nozzle. The mixing chamber was constructed with a 4.5”OD x 4” height 304 stainless steel pipe and two stainless steel plates welded on each end. Holes were drilled and tapped into the mixing chamber to allow for the gas inlet, the nozzle, a pressure gauge, and a thermocouple. This volume was heated using a 300W rope heater.

The gas temperature was held constant at 150 °C throughout the course of the experiments as change in fuel temperature can affect the NO_x generated. 150 °C was chosen as it was lower than the temperature reformate gas is often generated at, but was not low

enough such that the water would start to condense out. A lower temperature than standard reforming temperatures was chosen as the CH_4 that was not reformed would still be at ambient temperatures. In reality the temperatures of the gas mixtures would change based on reformate gas ratio, but temperatures were held constant to better identify the intrinsic emission characteristics of the blend.

3.5.4 Temperature Control

Omega 1/16” ungrounded k-type thermocouples were used to measure the fluid temperatures of the system. These thermocouples read the inlet and outlet temperatures of all the vaporizers, gas heaters, and mixing chamber. In addition to the heater temperatures, the nozzle temperature, inlet air temperature, and downstream exhaust temperatures were read. The thermocouples were fitted with ferrules to provide a seal at the mating surface to the fuel lines. For measuring surface temperatures, Omega 1/32” ungrounded k-type thermocouples were used. The surface thermocouples were coiled around the heating elements and were held in place with insulation.

To control the temperatures of the vaporizers, gas heaters, and mixing chamber a PID function was utilized. The PID function used the wall temperatures of the subsystems as the process variable and output a PWM signal. This PWM signal was sent to a Crydom solid state relay to modulate the mains voltage being sent to the heating elements. To keep the system temperatures consistent the gas lines and heaters were insulated using 1” Rockwool fixed to the system with steel wire.

3.5.5 Data Acquisition

During the course of the experiments there were two data acquisition systems used. For the first half of the first replication and for all shakedown experiments a National Instruments

SCXI-1000 and SCB-68 were used to read temperatures from the thermocouples, and voltages coming from the gas flow meters and NO_x sensor. These devices were controlled with a windows PC using Labview. The computer broke during the course of the experiments so a new system was built. For the remaining experiments, an Arduino Mega handled the data acquisition. Adafruit Max31855 cold junction compensated thermocouple amplifying modules were used to measure thermocouple data and an Adafruit ADS1115 16 bit ADC+PGA was used to read voltages from the flow meters and NO_x sensor.

3.5.6 Fluid Metering

The volumetric flow rates were monitored and controlled with two types of metering systems. The air being supplied to the system was metered and monitored with an Omega GFC67 mass flow controller. The H_2 and CH_4 were metered and monitored using Omega FMA5428 mass flow controllers. The CO and CO_2 blend, however, were controlled using analog rotameters with built-in needle valves. The meters are all calibrated from the factory using N_2 so k factors were applied to compensate for gasses used. As an added safety measure and to turn off gasses not in use, solenoid valves were placed upstream of the mass flow controllers and rotameters.

3.5.7 Emissions Measurement

The NOx sensor used was the California Analytic 400-HCLD. This system uses a chemiluminescent CLD gas analyser to determine NO_x content of sample gas. Due to faulty components on the motherboard of the system the reading had to be taken directly at the sensor. A calibration curve was created for the sensor using known span gas mixtures produced by Gasco. The NO_x sensor requires that the gas be dry and free of particulates. To achieve this the exhaust from the system was first passed into a sparge filter that was sitting in an ice bath.

This cools the gas to pull water out and filters out some of the particulate matter in the gas stream. The gas stream then flows over a Drierite desiccant bed to fully dry the gas.

3.6 Factorial Design of Experiments and Yates Data Analysis

The experimental data was analyzed using Yates method coupled with factorial analysis. Yates method takes a small number of results of a system and determines statistical significance of each of the independent variables and their interactions on the dependent variable.

The data will be analyzed with a two level, two factor model , known as a 2^2 model. This model assumes a linear relation over the range being tested. In a 2^2 model, each input will be given a high and a low configuration denoted with + and - symbols. The data set is composed of outputs from experiments run over all input parameter permutations. In a 2^2 model there are four distinct permutations that are tested, shown in Table 3.

Table 3. Factorial Design Run Configurations

Run	X1	X2
1	+	+
2	-	+
3	+	-
4	-	-

Once the required data was collected the effects and interactions of the tested variables could be calculated. The effect of a variable X1 is calculated using Eq 3.20

$$E_1 = \frac{\Sigma Y_{X1=+}}{n_{X1=+}} - \frac{\Sigma Y_{X1=-}}{n_{X1=-}} \quad (3.20)$$

In Eq. 3.20, Y represents the output variable and n is the number of high or low parameters in the specific configuration.

To determine the statistical significance of the effects calculated, a signal to noise ratio needs to be calculated. In order to complete this step at least two replications, denoted as r, of the study must be conducted. This first step in calculating a signal to noise ratio is determining the variance in measurements for each configuration. Each variance, s^2, is calculated using Eq 3.21

$$s^2 = \sum_{i=1}^{r} (Y_i - \overline{Y})^2/(r - 1) \quad (3.21)$$

From here the pooled variance is derived by taking the mean of all the individual variances. The square root of the pooled variance is the pooled standard deviation. The standard error can then be calculated with Eq 3.22.

$$S_E = \frac{\sigma_p}{\sqrt{n_f}} \quad (3.22)$$

Where σ_p is the pooled standard deviation and n_f is the number collected of data points. The standard error is used to calculate the signal to noise ratio through Eq 3.23.

$$t_E = \frac{Effect}{S_E} \quad (3.23)$$

t_E is calculated for each effect and interaction. The significance of each effect and interaction can then be evaluated by comparing an effects specific t_E to a critical t-value, t*. The value of t* is found from a student-t two tail distribution table. The value of t* is dependent on the number of degrees of freedom in the system as well as the confidence level desired. In the case of a 2^2 model with three replications, there are eight degrees of freedom.

3.7 Shakedown

To determine the operating limits of the combustion as well as verify functionality of the experimental system preliminary experiments were conducted. These preliminary experiments, referred to as shakedown, started by running a pure methane flame in the system at varying mass flow rates. This allowed for the confirmation that heating systems were working, the emissions analyser was properly taking data, and that the chosen flow rate was reasonable for the system. Next, shakedown experiments were run with reformate gas blends to determine where in the design space the flame started to become unstable. Unstable in this case was defined as the flame lifting off the nozzle or extinguishing. During this stage it was found that the vaporization of water was not steady enough to get accurate results. These unsteady vaporization events are commonly called surging. Surging in this experiment would cause there to be too little water in the fuel for extended periods of time and far too much water for brief periods of time. To illustrate this problem more a plot of NO_x vs time for a system with high surging is shown below in Figure 9. During shakedown surging proved to be a major challenge as the large differences in water content would drastically change the emissions as well as often extinguish the flame. The flame extinctions would most commonly occur during tests that had high steam to carbon ratios and low reformate gas ratios. This corresponds with trends observed in Hwang's "*Blowout and Emissions Characteristics Evaluation of Methane Steam Reformate Gas*" [11]. In this study it was found that the addition of reformate gas significantly increased the flame stability when added to a methane flame. The increased flame stability in high reformate gas ratio flames allowed the flame to continue to burn even in very high water content scenarios, whereas the low reformate content flames were extinguished in these situations.

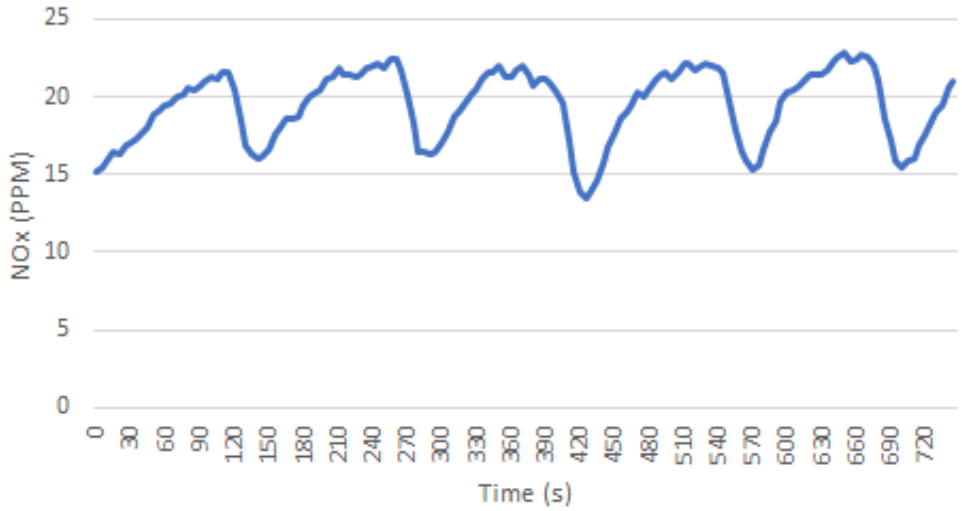

Figure 9. High Surging Example

The surging was most likely caused by a phenomena known as superheating or boiling delay. In systems with very low flow rates and a lack of nucleation sites, such as in the vaporizer, water can be heated to above its boiling point [26]. Once some of the superheated water eventually vaporizes, the nucleation sites generated by the vapor allow the rest of the superheated water to quickly vaporize.

To address this issue the initial vaporizer was set to only 90 °C to act only as a preheater. The bulk of the vaporization then took place further down the heating system where the water would be separated into large droplets. Additionally, the steam to carbon ratio range was chosen such that the surging effect was minimized. The results of altering these parameters can be seen in Figure 10. below.

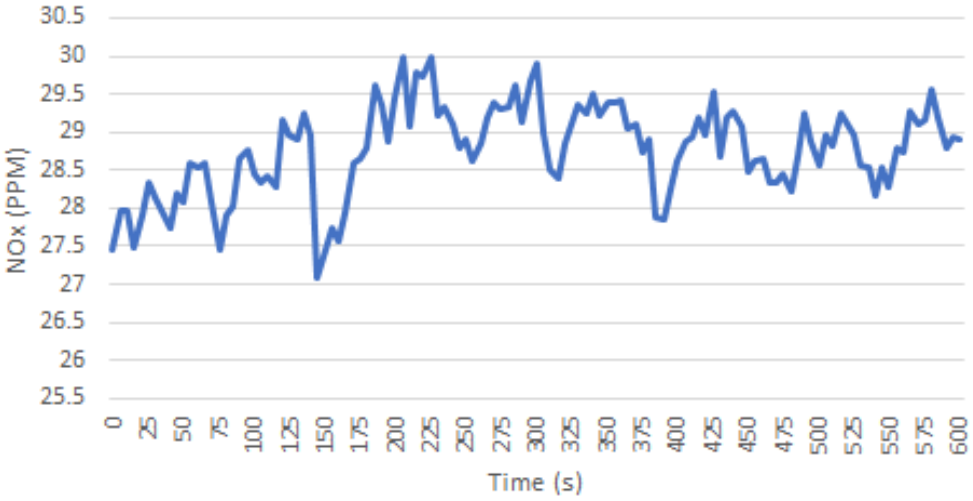

Figure 10. Reduced Surging Example

3.8 Procedure

The first step in preparing the system for operation was turning on the NO_x sensor. The sensor took approximately 60 minutes to heat up and reach steady state, so it was allowed the most time to start. The next step in the process was connecting all the gas lines to the required inputs to the system. The shop air regulator was set to 200 kPa and lines were run to the emissions analyser as well as to the mass flow controller metering the air. Once the gas analyser was warmed for sufficiently long, it was zeroed. The gas bottles were opened at this point to verify sufficient gas levels for the planned experiments. Regulators on the gas tanks were then set to 200 kPa.

To preheat the chamber and gas lines, a steady flow of 10 SLPM of CH_4 was run through the lines and was burned in the combustion chamber. This was allowed to preheat until all temperatures being read were stabilized at the desired values. At the end of this warm-up procedure the system was ready to start collecting data.

Throughout the course of the experiments the volumetric flow rate was fixed to 10 liters per min. 10 liters per min was chosen as it was close to the highest flow rate that was found in shakedown that did not result in the flame lifting off in any configuration. The volumetric flow rate was held constant to fix the jet velocity at the nozzle. To avoid error from hysteresis and to determine error in the measurements of the system, three replications of the experiment were done with order of configurations changed between replications.

During shakedown, configurations were allowed to run for varying sets of time. After approximately ten minutes there was little change in the system. So, between configurations during official data collection the system was allowed to reach steady state for ten minutes. After this period, the data was collected for an additional ten minutes.

Gas was pre heated to 150 °C to simulate the hot reformate gas being added to the fuel stream as well as to keep the water vaporized. The first stage of the vaporizer was set to 90 °C. This stage acted to preheat the water and get it as close to boiling as possible. From there, the preheated liquid water was added through a 0.25” tee into the 150 °C gas stream right before the second gas heater. As the small volumes of water were physically separated from one another with gas at the time of vaporization there was a lesser chance of large simultaneous vaporization events. These large vaporization events were what was causing the surging in the shakedown experiments.

3.9 OpenFOAM 2D Simulation

The open-source program OpenFOAM was chosen to do preliminary investigations on the burning and emission characteristics of the fuel blends that were to be tested. The simulation was built on the ReactingFoam sub-program and used the GRI-3.0 mechanism to compute the chemical kinetics. The seulex solver, a linearly implicit Euler method with step size

control and order selection, was chosen as the ODE solver as it was one of the less computationally expensive solvers that had adaptive step size and could handle the relatively stiff system effectively. The model did not use any turbulent flow models and utilized laminar flow approximations for flow solutions. While this was not ideal, simplifications had to be made in order to solve the simulations on the computer available. To improve the accuracy of the system while using laminar flow approximations, the flow rates of the fuel and air were lowered compared to the experimental system. This should not have too large of an impact on the final emissions as the results are normalized. The gas inlet concentration values were calculated such that the volumetric flow rate through the nozzle was constant. This was done to most accurately match how the experiment was run. The velocities input for the fuel and air were 1m/s and 0.1m/s respectively.

A reactor geometry was first created based on the burner housing set up in the lab. This model is displayed in Figure 11. Included in this model was a 0.64mm nozzle for fuel and a plane for co-flow air input evenly from the surface below it. In addition, the reactor measured 1370mm long to best model the real system.

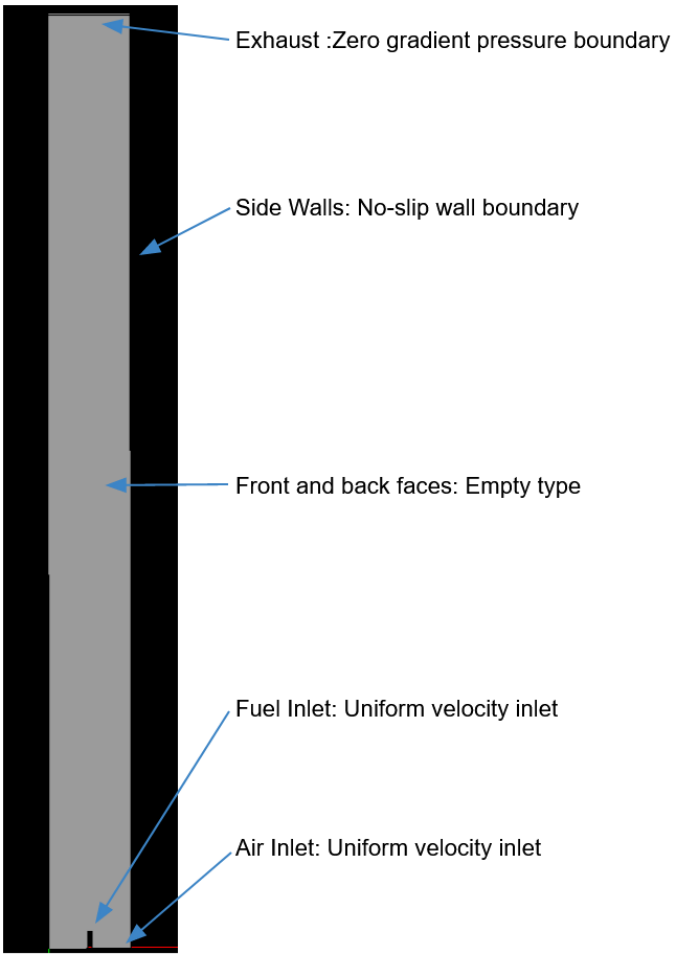

Figure 11. 2D Model Used for Simulation

The model was first modeled in Solidworks, but was meshed using Salome. The NETGEN 1D-2D algorithm was chosen to convert the 3D model into a mesh that could be solved as a 2D system. To determine a sufficiently fine mesh a test case of a pure methane flame was run for 2 simulated seconds. The average NO_2 at the outlet was used as the goal to determine mesh convergence. NO_2 emissions were evaluated by reading the average concentrations at the outlet boundary. The model was considered converged when there was a less than 1% difference between mesh configurations. The mesh incorporated mesh refinement regions located around the nozzle and in the base of the flame structure. Each mesh refinement level shown in Figure 12. halved the cell boundary lengths, approximately quadrupling the

number of cells in the mesh. The minimum mesh size in the final simulations had edge lengths of 0.2 mm in the refined regions and contained over 330,000 cells.

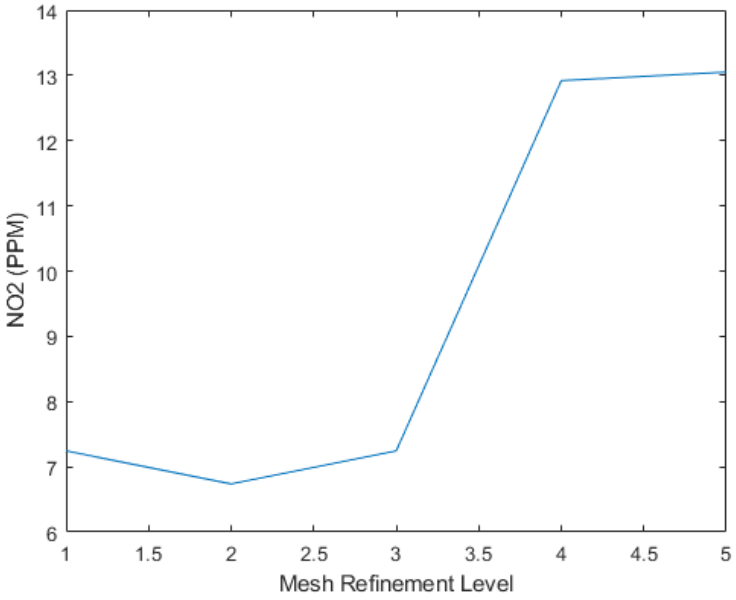

Figure 12. Mesh Refinement Study

The ReactingFOAM sub-program was based on a transient solver. To get steady state solutions the simulation had to be run over many time steps until reaching a defined time at which steady state was assumed. During the simulations of the test case, time steps of 0.1 second were evaluated in order to determine the time required to reach steady state. The system reached steady state in 4 simulated seconds as shown in Figure 13. Between 4 seconds and 5 there was less than a 0.1% relative change in NO_2 output.

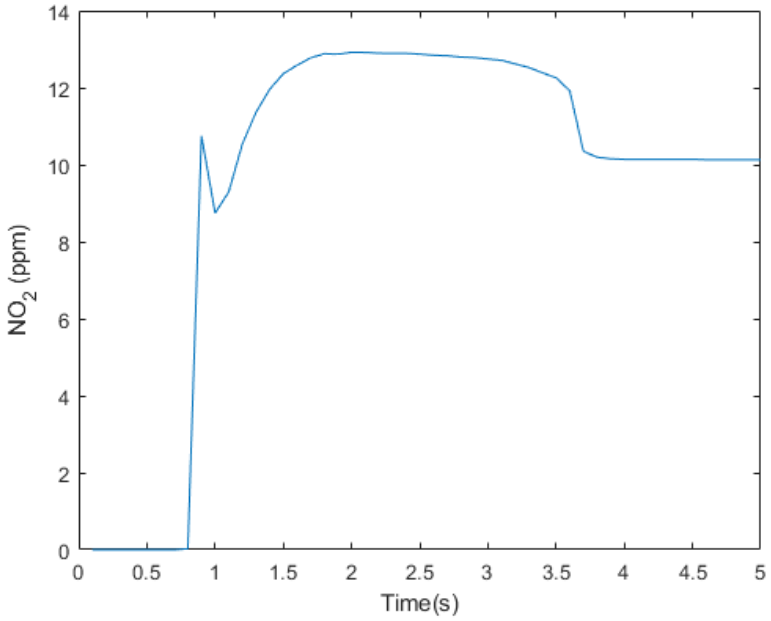

Figure 13. Time convergence of model

The slight plateau and final convergence of the time convergence model, Figure 13, was a result of how the models were initialized. It was found that when starting from a uniform reaction vessel the simulation would take approximately 2.5 seconds to reach steady state. when, however, the model was initialized using the final result of the pure methane flame, then the model would only need to be run for 2 additional seconds before reaching steady state. So all configurations started at 2 seconds using the results from the mesh convergence study as the initial model state. Then simulations were run for 2 more seconds to reach the steady state of the tested fuel blend.

Chapter 4

Results and Discussion

4.1 Simulation Results

Nine configurations of the input parameters were tested over the same range as the experiment to show general trends in the emission characteristics of the reaction. These configurations were even spaced throughout the design space and aligned with configurations experimentally tested. An example single configuration result is shown below in Figure 14.

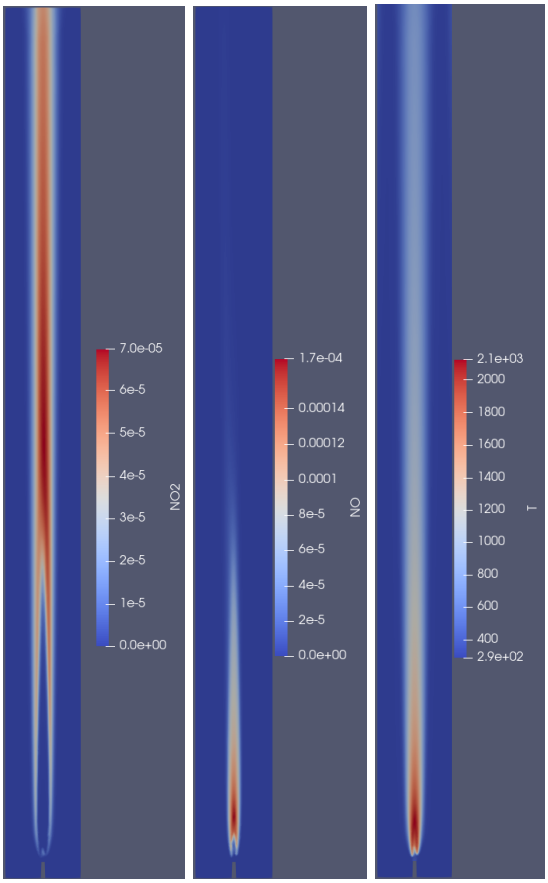

Figure 14. NO_2 Molar Ratio (left) NO Molar Ratio (middle) and Temperature (K) of the 12.5% Reformate gas flame and 2 Steam to Carbon Ratio Configuration

To compare the results to the experiment the average NOx values at the outlet of the simulation were normalized to be in terms of nanograms of NO_x per Joule of CH_4. The results of the post processing are displayed in Figure 15.

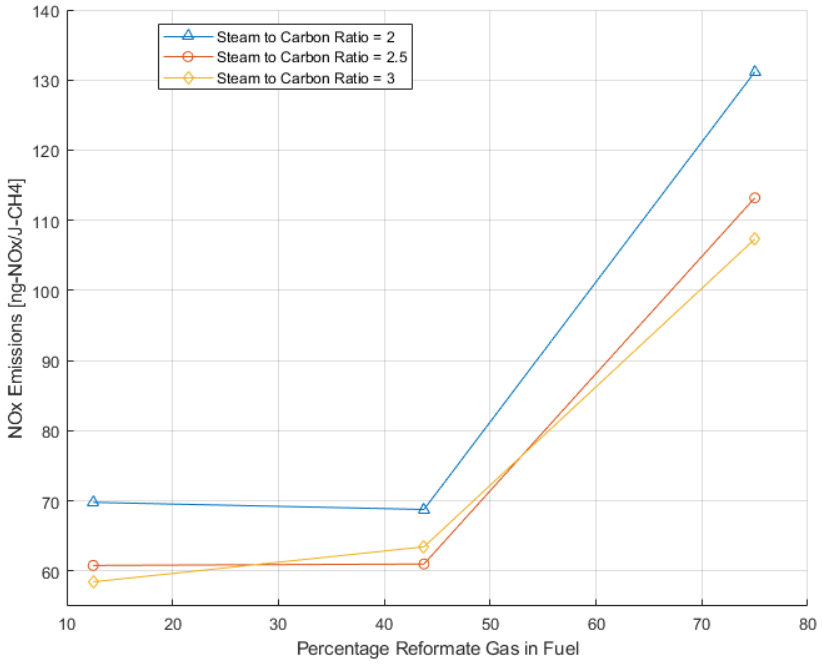

Figure 15. Simulation results

The first major trend visible in Figure 14. is that the NOx emissions are highly dependent on the reformate gas content of the fuel. When the reformate gas content in the fuel increased, over the span of the tested parameters, the NO_X generated increased. The steam to carbon ratio also altered the NO_X output of the system, however, not as substantially as the reformate gas ratio. The other trend found in Figure 15. is that the emissions were not linearly based on either the reformate gas ratio nor the steam to carbon ratio. Between 12% and 43% reformate gas there was little change in the emissions, but increasing the reformate gas ratio further drastically increased the NO_X. As the Zeldovich mechanism for NO_X generation is highly dependent on temperature, the peak temperatures of the configurations were investigated and are displayed in Figure 16.

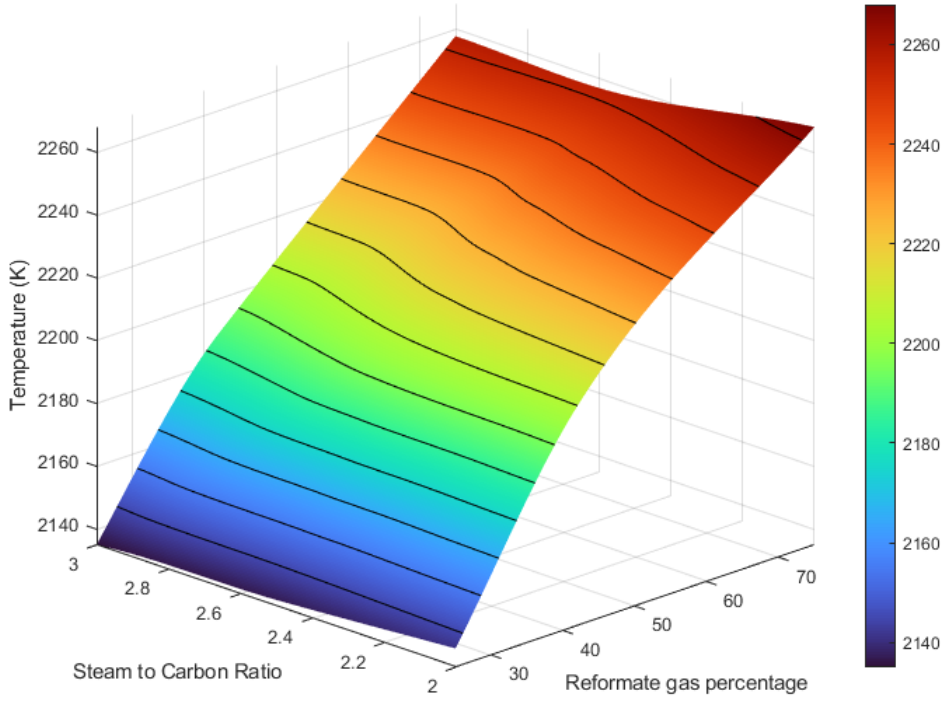

Figure 16. Peak Temperature of Simulated Flame

While the NO_X emissions were nonlinear, the peak flame temperatures of the configurations were fairly linear. There are a handful of explanations on why the NO_X would be significantly nonlinear with a linear change in temperature. The first of which is that the Zeldovich mechanism is nonlinear. While this doesn't explain the small change in NO_X emissions over the lower half of the reformate gas ratio range, it describes why the system acted nonlinearly. Another aspect of the system that caused some nonlinearity was that the mass flow rate of fuel going into the system was changed with each configuration. While the mass flow rate won't significantly affect the flame temperature it would affect the amount of nitrogen in the air that was heated to the point at which the Zeldovich mechanism is significant.

4.2 Experimental results

Six levels of reformate gas concentrations were tested at five levels of steam to carbon ratios. This resulted in 30 data points being taken for every replication. The data set was replicated three times. Such a large quantity of data was collected to allow for the ability to perform data analysis, such as curve fitting, for any specific parameter holding the other parameter constant. Previous research had shown a linear relationship between reformate gas ratio and NO_x emissions over a large range but a nonlinear result was expected based on the simulation.

Figure 17 below shows the normalized NO_x emissions of the system vs the reformate gas content at a given steam to carbon ratio. This data was derived from the mean of each datum over the three replications. The major trend shown in this figure is that the emissions increase non-linearly with the inclusion of reformate gas.

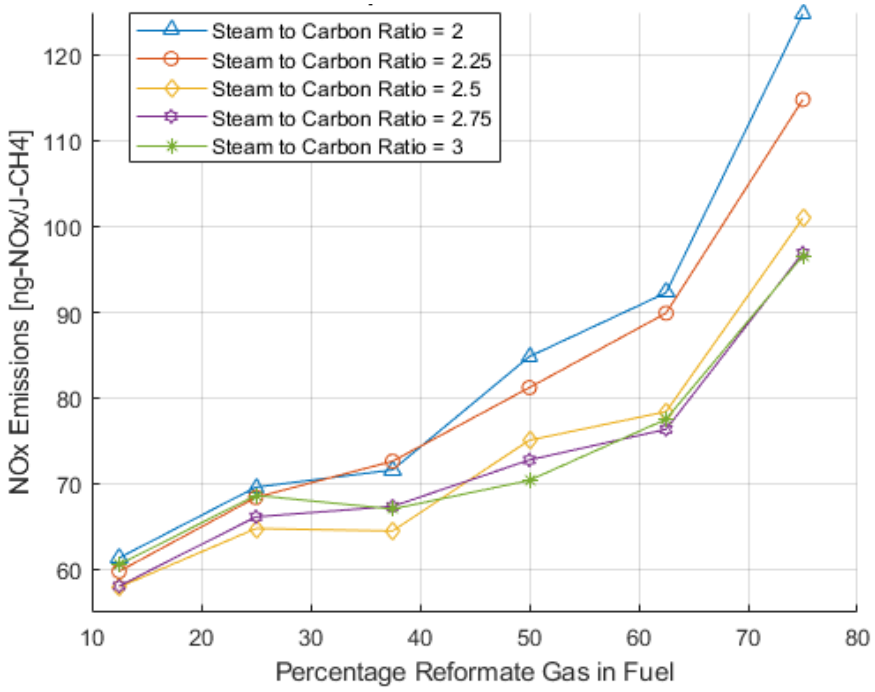

Figure 17. NO_x Emissions vs. Fuel Composition Experimental

While reformate gas content in the fuel was positively correlated to an increase in NO_x emissions, the steam to carbon ratio was negatively correlated, as shown in Figure 18. When taking into account the error associated with the results, the emissions appear to linearly decrease with the addition of water in the fuel.

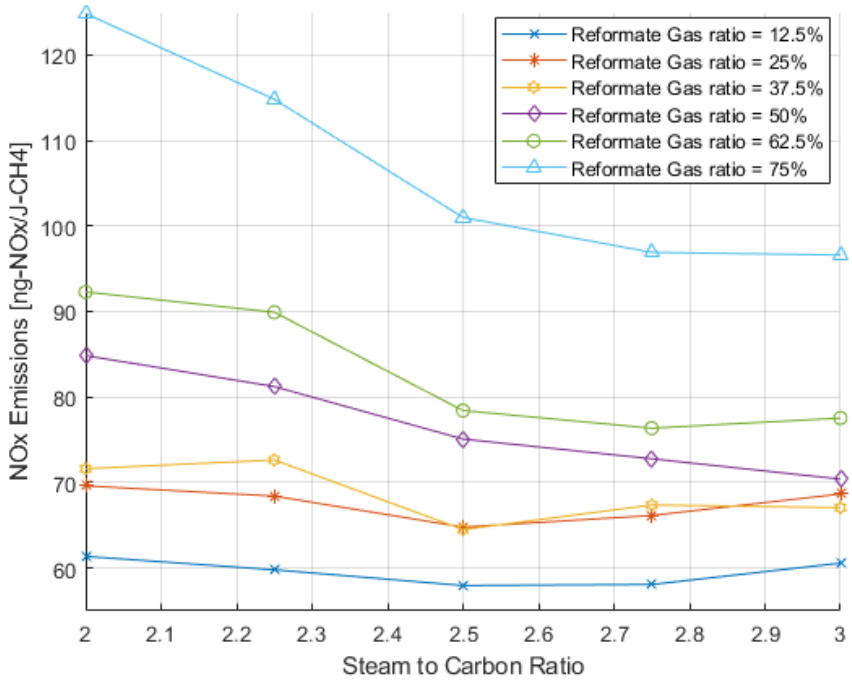

Figure 18. Steam to Carbon Ratio vs. NO_x Emissions

To illustrate the error in the results, the plot of NO_x vs reformate gas ratio for a steam to carbon ratio of 2 is plotted below in Figure 19. This figure includes error bars that are two standard deviations in total length, where the standard deviation over the three replications is calculated for each individual data point.

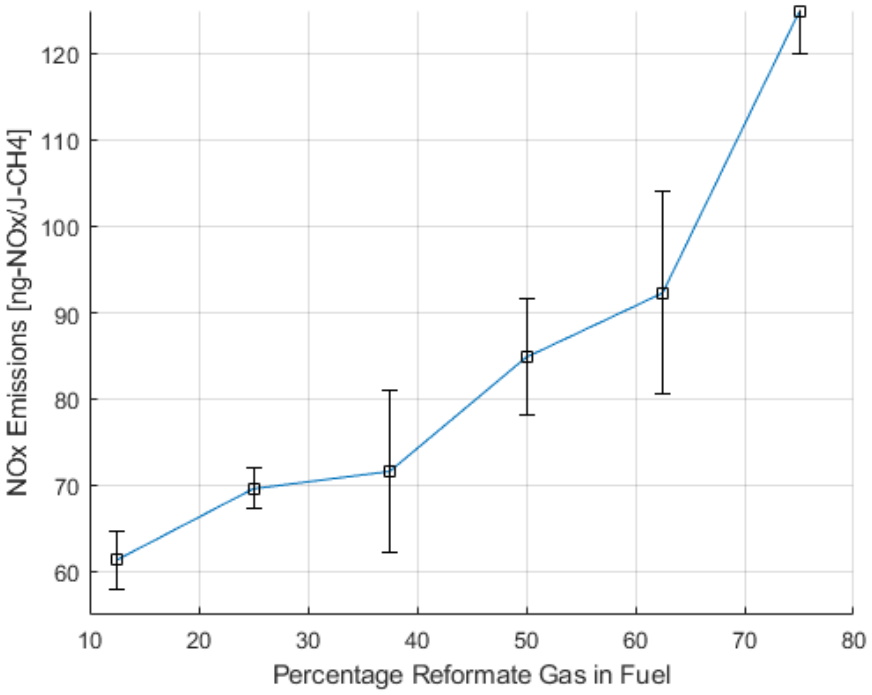

Figure 19. NOx Emissions vs. Fuel Composition with Error Bars

The large standard deviations displayed in Figure 19. are most likely a result of some surging in the system. The water content in the fuel fluctuated over time due to large vaporization events taking place in the vaporizers. Even though the error bars are large, the general trend of a non-linear increase in emissions based on reformate gas content is still visible.

Figure 20. best illustrates that the addition of reformate gas increases the relative emissions characteristics of the system for all steam to carbon ratios in the defined design space. This trend was also present in Figure 15. and Figure 21. below in the simulated results. The surface plot shown in Figure 20. is an interpolated surface generated from the average experimental data collected, however, the original measure data points are plotted on this surface and are denoted with a X.

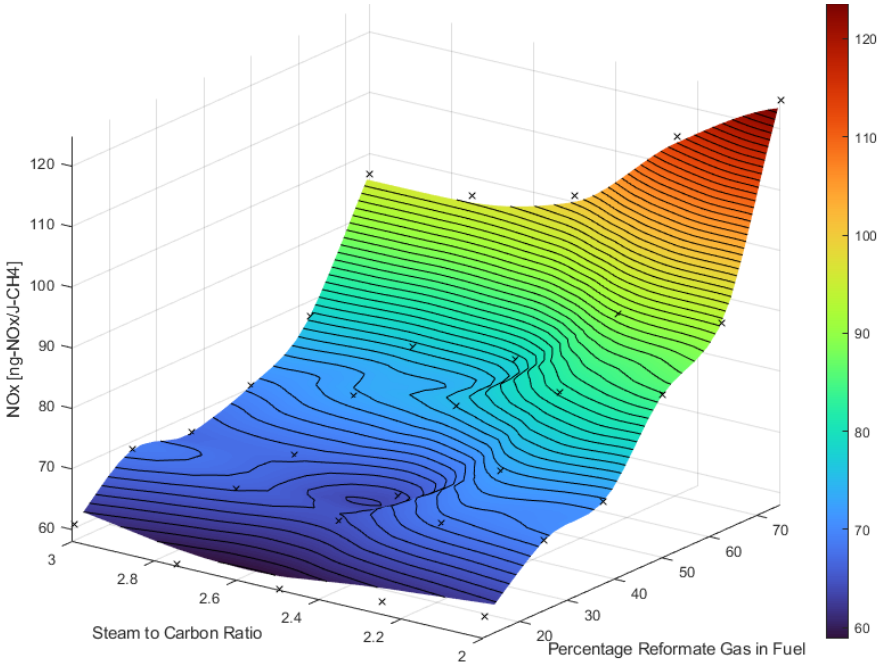

Figure 20. Experimental 3D NO_x Emissions vs. Fuel Composition

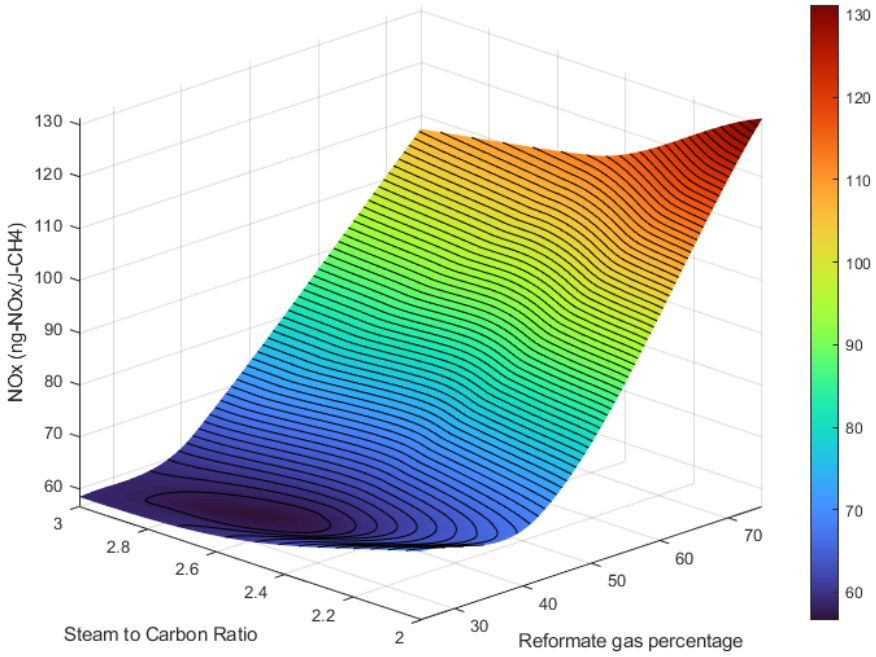

Figure 21. Simulated 3D NO_x Emissions vs. Fuel Composition

To best compare the experimental and simulated results, matching groups of configurations are plotted against each other in Figure 22.

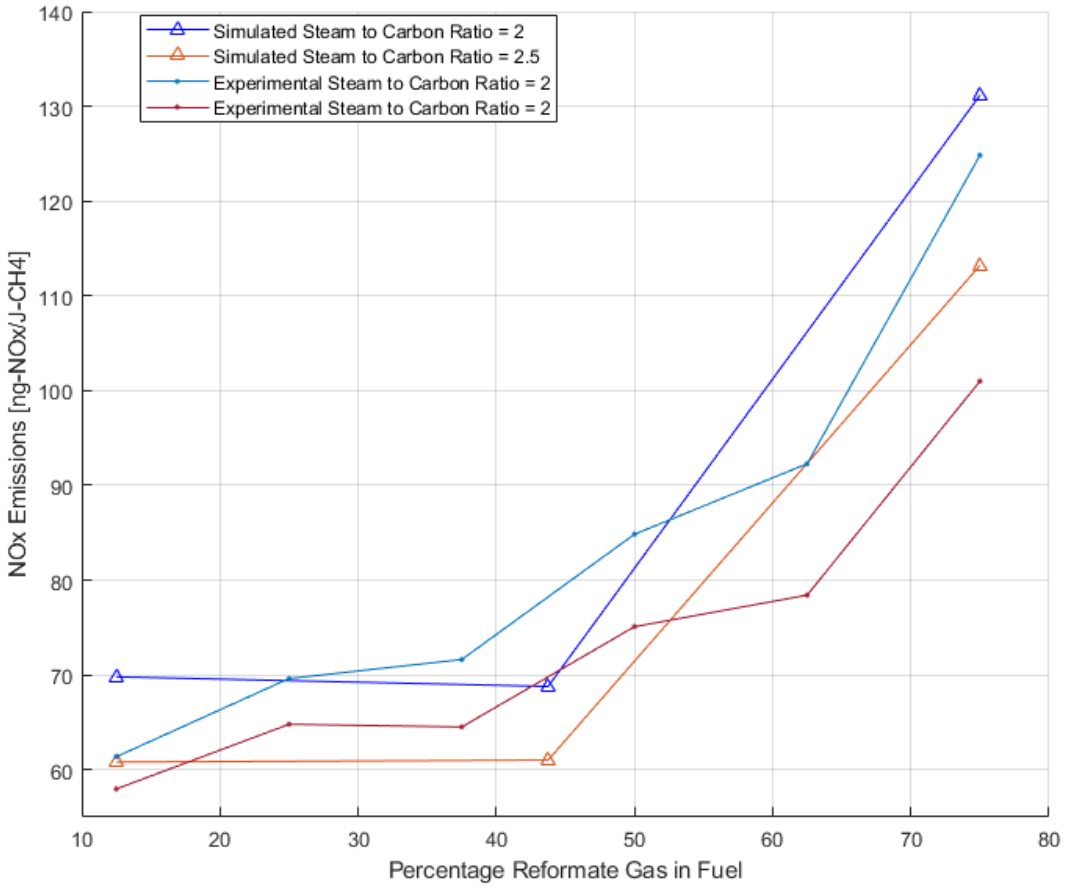

Figure 22. Simulated vs. Experimental Results

The simulation and the experiment appeared to generally match one another. Both methods of analysis displayed nonlinear relationships between the two independent variables and the NO_X emissions generated. In addition to this, the emissions reported by each method differed by approximately 10%-15% for each configuration. The simulation tended to report a higher NO_X reading on average than the experimental data presented.

A two level two factor factorial design was created across the maximums of the design space. Although more data was collected, only a two level study was done as a two level model was sufficient to show significance over the tested range. The two level model also generated parameters detailing the impact each of the variables had on the system. The results pulled from the data for Yates analysis are displayed in Table 4. below where X1 is reformate gas percentage and X2 is steam to carbon ratio.

Table 4 Experimental Results

Configuration	Setting		Value		Y [ng/J]]			Avg Y	Variance	% error
	X1	X2	X1	X2						
1	+	+	75	3	95.2	103.8	88.0	95.6	62.7	8.28%
2	-	+	12.5	3	59.0	66.9	60.1	62.0	18.5	6.94%
3	+	-	75	2	124.9	118.6	126.1	123.2	16.3	3.28%
4	-	-	12.5	2	64.2	59.3	65.7	63.1	11.4	5.35%

Using the data shown above in Table 4., the pooled mean, variance, and standard error were calculated. The results are displayed in Table 5.

Table 5.

Pooled Mean	Pooled Variance	Standard Error	Degrees of Freedom	t* at 99% Confidence	t* at 99.9% Confidence
85.97	27.23	3.0125	8	3.355	5.041

The resultant values were then input into the equations described in Chapter 3 section 6 to calculate the effects and interactions of the system. Table 6. displays the effects, interactions, and their significance over the design space.

Table 6. Effects and Significance

	X1	X2	X1X2
Σ+ - Σ-	93.8	-28.6	-26.5
Effect or Interaction	46.9	-14.3	-13.2
Signal to Noise t-ratio	15.6	-4.7	-4.4
Significant at 99%	Yes	Yes	Yes

In this range, the reformate gas concentration greatly increased the nitrogen oxides present in the exhaust stream. Water content in the fuel, however, significantly decreased the nitrogen oxide emissions to a lesser degree.

4.3 Observations

Over the course of experimentation the system extinguished itself frequently. The main cause of this extinction was surging taking place, increasing the water content in the fuel. The high reformate gas content flames never blew out during surging events, however, low reformate content flames blew out often. This seems to suggest that the reformate gas added significant flame stability to the system.

The difference in flame color and length was drastically altered by both the water content as well as the reformate gas content in the fuel. These differences are illustrated in Figure 23 and 24.

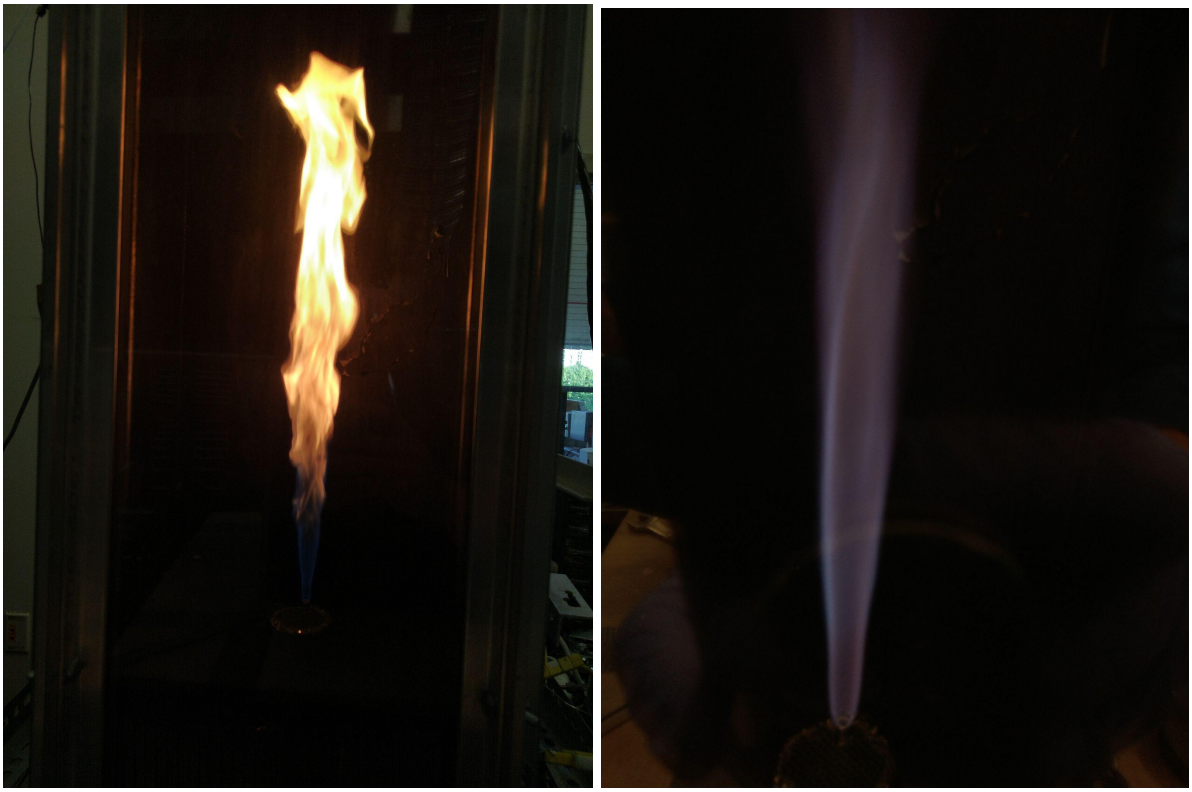

Figure 23. Low Reformate and Low Water Content Flame (Left) and High Reformate and Low Water Content Flame (Right)

As shown in Figure 23. the color of the flames for the high methane content configurations were yellow to red. The flames, additionally, tended to be the longest, most turbulent, and most likely to extinguish during surging events. The high reformate gas content flames were much dimmer than the high methane flames. The color was much more blue, but still had red undertones, especially at high steam to carbon ratios as shown in Figure 24. At the highest reformate gas concentration, the length of the flame was approximately half the length of the lowest reformate concentration flame.

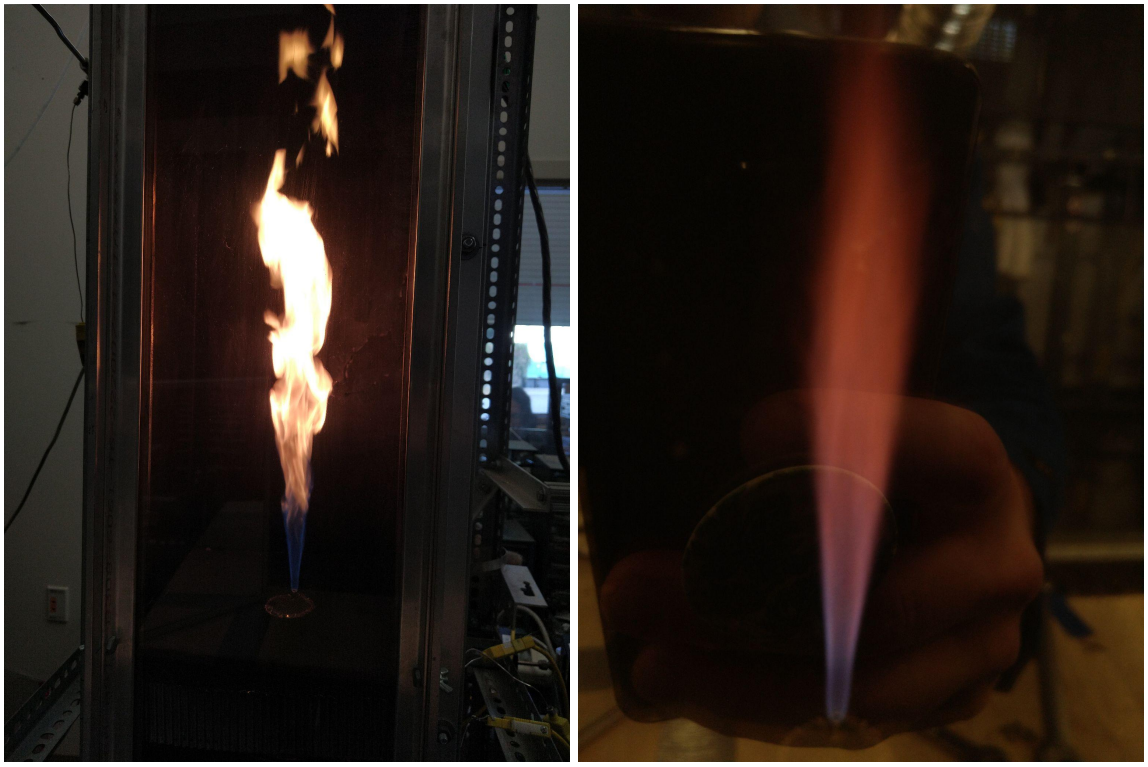

Figure 24. Low Reformate and High Water Content Flame (Left) and a High Reformate and High Water Content Flame (Right)

The steam to carbon ratio of the flame also made significant changes to the flames appearance. The changes were most significant at high reformate gas concentrations. At high reformate gas concentrations the added water would alter the flame color from being uniformly blue to being purple and red. This was most likely due to the lower temperatures reached by the flame.

Chapter 5

Conclusion and Recommendations

In conclusion, non-premixed, reformate-methane flame was experimentally and numerically investigated to explore the effect of steam to carbon ratio and reformate gas content on the emissions generated. To achieve this the steam to carbon ratio was varied from 2 to 3 while the reformate gas content was varied from 12.5% to 75% on a molar basis. Nitrogen oxide measurements were collected and analyzed to determine trends throughout the design space. An OpenFOAM simulation was additionally created to model the flame produced by gas blend . Both the experiments and simulations concluded that a reformate-methane bi-fueled diffusion flame operating in a laminar coflow air setting will produce more NO_x emissions than a pure methane flame would. Inversely water content, or steam to carbon ratio, was shown to significantly reduce NO_x emissions.

In the future, there are many further experiments that could be conducted to further investigate this topic. The first of these research options is investigating the combustion characteristics of reformate-methane blends when burning premixed and lean. As observed, the reformate gas increases flame stability, which should allow the flame to be burned leaner. This leaning of the flame would decrease flame temperatures, most likely decreasing the NO_x emissions. As the lean limits were only tested with the addition of water in this experiment it would be valuable to investigate if air dilution would yield similar results. From observations made in this experiment higher reformate gas ratios should allow for the use of leaner premixed systems.

Another possible study could investigate how the emissions would change when implemented in a real turbine. A turbine would operate at far higher pressures and inlet

temperatures than those tested in this experiment. In addition to this, the residence time of hot nitrogen and oxygen in the system would be reduced when compared to this study. Both the temperature and residence time would significantly affect the formation of NO_x.

Appendix A

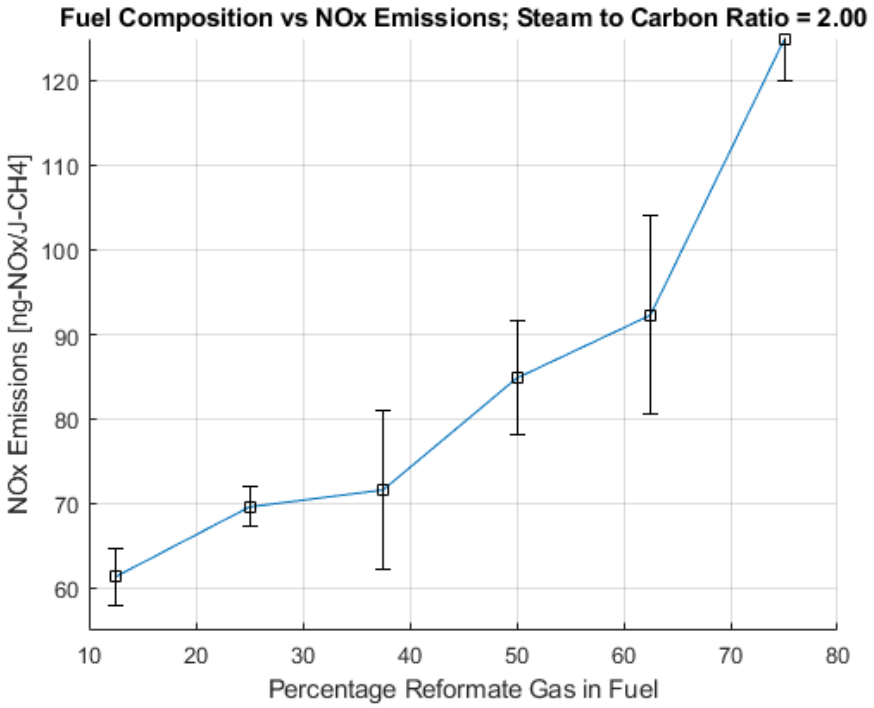

Figure A1.

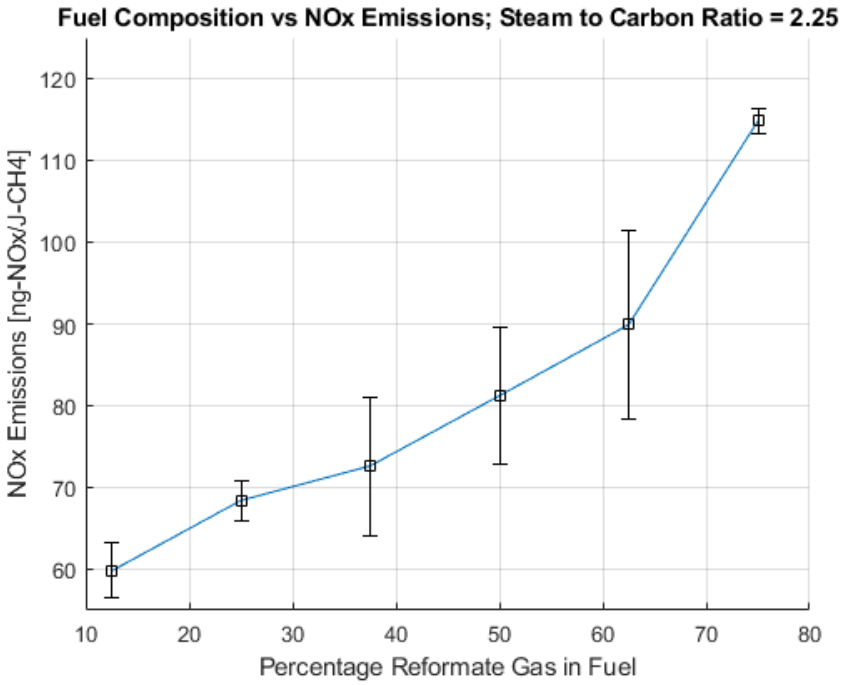

Figure A2.

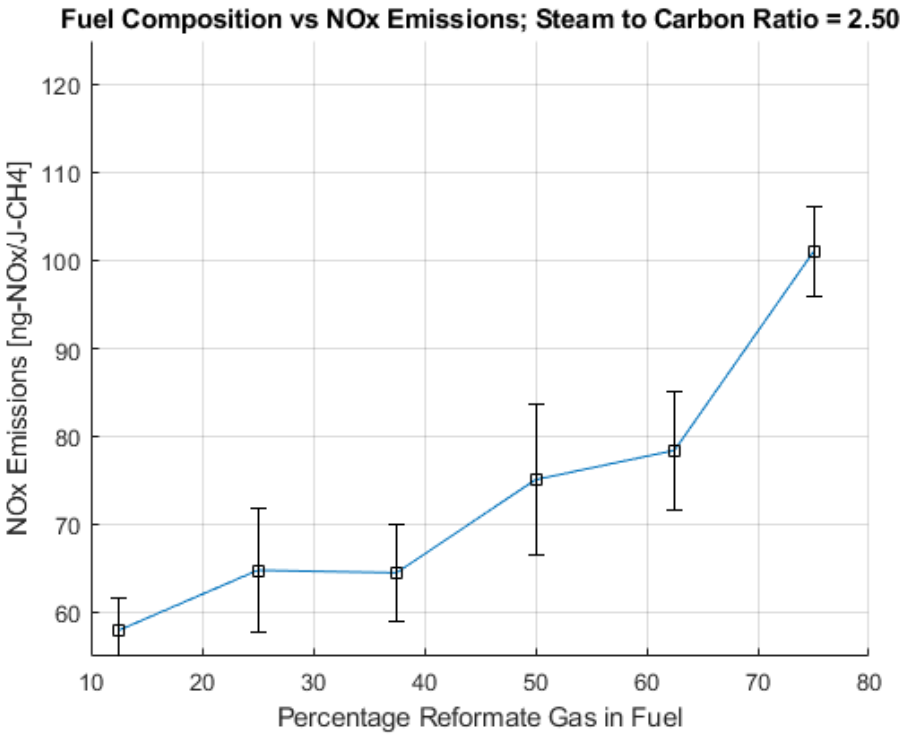

Figure A3.

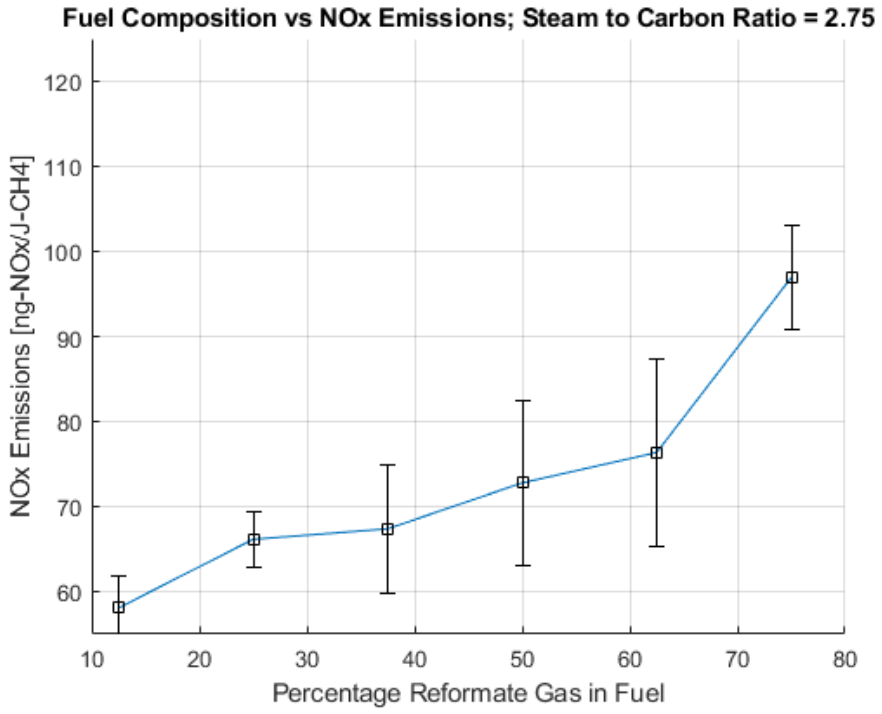

Figure A4.

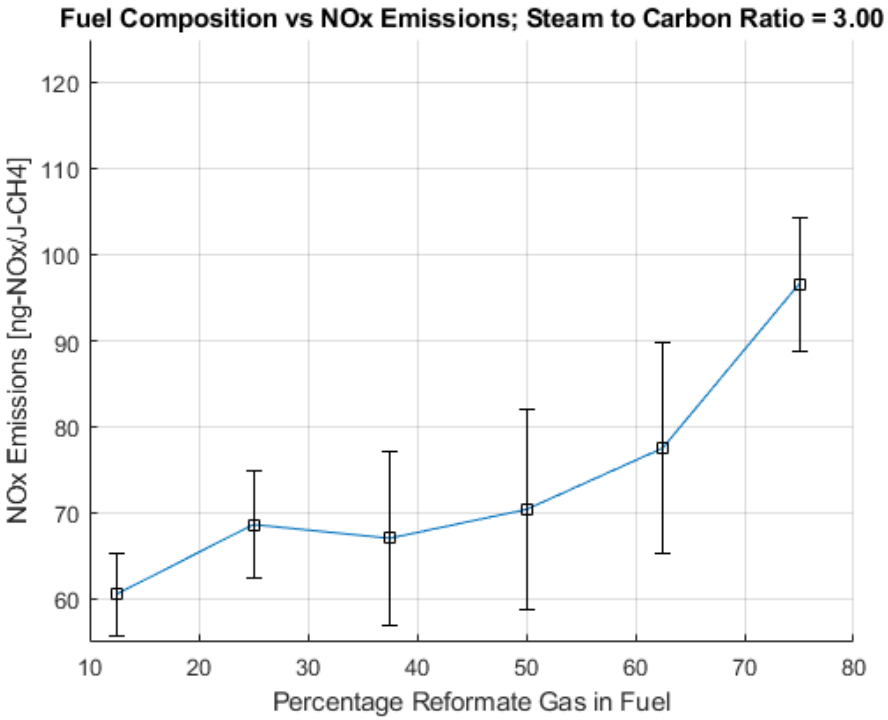
Fuel Composition vs NOx Emissions; Steam to Carbon Ratio = 3.00
NOx Emissions [ng-NOx/J-CH4]
120
110
100
90
80
70
60
10
20
30
40
50
60
70
80
Percentage Reformate Gas in Fuel

Figure A5.

Bibliography

[1] U.S. Energy Information Administration. 2022. *Annual Energy Outlook 2022 with projections to 2050*. [online] Available at: <https://www.eia.gov/outlooks/aeo/pdf/AEO2022_ChartLibrary_full.pdf> [Accessed 19 July 2022].

[2] 2012. *AP-42, Vol I, 3.1 Stationary Gas Turbines*. [online] Available at: <https://www3.epa.gov/ttnchie1/ap42/ch03/final/c03s01.pdf> [Accessed 19 July 2022].

[3] 2012. *40 CFR Part 60 Standards of Performance for Stationary Gas Turbines; Standards of Performance for Stationary Combustion Turbines; Proposed Rule*. [online] Available at: <https://www.govinfo.gov/content/pkg/FR-2012-08-29/pdf/2012-20524.pdf> [Accessed 19 July 2022].

[4] 2006. *The Gas Turbine Handbook*. U.S. Department of Energy Office of Fossil Energy.

[5] 2001. *Gas Turbine Emissions and Control*. [online] Available at: <https://www.ge.com/content/dam/gepower-new/global/en_US/downloads/gas-new-site/resources/reference/ger-4211-gas-turbine-emissions-and-control.pdf> [Accessed 19 July 2022].

[6] Schefer, R. W., “Hydrogen enrichment for improved lean flame stability,” International Journal of Hydrogen Energy, Vol. 28, No. 10, 2003, pp. 1131–1141.

[7] Juste, G., “Hydrogen injection as additional fuel in gas turbine combustor. Evaluation of effects,” International Journal of Hydrogen Energy, Vol. 31, No. 14, 2006, pp. 2112–2121.

[8] Frenillot, J. P., Cabot, G., Cazalens, M., Renou, B., and Boukhalfa, M. A., “Impact of H2 addition on flame stability and pollutant emissions for an atmospheric kerosene/air swirled flame of laboratory scaled gas turbine,” International Journal of Hydrogen Energy, Vol. 34, No. 9, 2009, pp. 3930–3944.

[9] Maughan, J., Bowen, J., Cooke, D., and Tuzson, J., “Reducing gas turbine emissions through hydrogen-enhanced, steam-injected combustion,” Journal of Engineering for Gas Turbines and Power , Vol. 118, No. 1, 1996, pp. 78–85

[10] Öztuna, S., Kemalettin Büyükakın, M., “Effects of hydrogen enrichment of methane on diffusion flame structure and emissions in a back-pressure combustion chamber” International Journal of Hydrogen Energy, Vol. 45, No. 10, pp. 5971-5986

[11] Hwang, Jungyu.,“Blowout and Emissions Characteristics Evaluation of Methane Steam Reformate Gas”, Dissertation

[12] Züttel, A., “Hydrogen storage methods”, The Science of Nature, Vol. 91, pp. 157–172

[13] Zhou,L., “Progress and problems in hydrogen storage methods”, Renewable and Sustainable Energy Reviews, Vol. 9, No. 4, pp. 395-408

[14] Ursua, A., Gandia, L. M.,Sanchis, P., "Hydrogen Production From Water Electrolysis: Current Status and Future Trends" , *Proceedings of the IEEE*, vol. 100, no. 2, pp. 410-426, Feb. 2012, doi: 10.1109/JPROC.2011.2156750.

[15] Hewson, J.C., Williams, F.A., “Rate-ratio asymptotic analysis of methane–air diffusion-flame structure for predicting production of oxides of nitrogen”, Combustion and Flame, Vol. 117, No. 3, pp. 441-476

[16] Basile, A., Liguori, S., Iulianelli, A., “Membrane reactors for methane steam reforming (MSR)”,Woodhead Publishing Series in Energy, pp. 31-59

[17] Kirk-Othmer, 1999. Concise Encyclopedia of chemical technology, Vol. 12, New York

[18] Warnatz, J., “The structure of laminar alkane-, alkene-, and acetylene flames,” Symposium (International) on Combustion, Vol. 18, No. 1, 1981, pp. 369–384.

[19] Y.B. Zel'dovich, 1946. "The Oxidation of Nitrogen in Combustion Explosions". Acta Physicochimica U.S.S.R. 21: 577–628

[20] 2014. The San Diego Mechanism Chemical-Kinetic Mechanisms for Combustion Applications. [online] Available at: https://web.eng.ucsd.edu/mae/groups/combustion /mechanism.html [Accessed 19 July 2022].

[21] Smith, G., Golden, D., Frenklach, M., Moriarty, N., Eiteneer,B., Goldenberg, M., Bowman, C., Hanson, R., Song, S., Gardiner, W., Lissianski, V., Qin, Z., “GRI-Mech 3.0” [online] Available at: “http://combustion.berkeley.edu/gri-mech/”

[22] Glassman, I., Yetter, R. and Glumac, N., 2015. “Combustion*”*. Amsterdam [etc.]: Elsevier.

[23] James, A.W.,.Rajagopalan, S., 2014 *Structural Alloys for Power Plants*, pp. 3-21

[24] Sanusi, Y. S., Habib, M. A., and Mokheimer, E. M. A. (October 23, 2014). "Experimental Study on the Effect of Hydrogen Enrichment of Methane on the Stability and Emission of Nonpremixed Swirl Stabilized Combustor." ASME. *J. Energy Resour. Technol*. May 2015; 137(3): 032203.

[25] Richards, O, Nadia., “Hydrogen Production Enhancement Using a Stratified Catalyst Bed in Reforming Systems”, Dissertation

[26] Debenedetti, P.G., 1996. “Metastable Liquids: Concepts and Principles”; Princeton University Press: Princeton, NJ, USA